

## **Journal of Quaternary Science**



Check for updates

## New age-estimate data and implications for marine isotope stage 7 and 5e sea levels in Fenland, eastern England

H. E. LANGFORD,  $^{1*}$   $\bigcirc$  M. D. BATEMAN,  $^{2}$  R. M. BRIANT,  $^{1}$   $\bigcirc$  D. J. HORNE,  $^{3,4}$  K. L. KNUDSEN,  $^{5}$  K. E. H. PENKMAN,  $^{6}$  L. WHEELER  $^{6}$  and J. WHITTAKER  $^{4\dagger}$ 

Received 16 March 2025; Revised 22 September 2025; Accepted 7 October 2025

ABSTRACT: Only one last interglacial relative sea-level indicator point (SLIP) has been recognised for Fenland, eastern England, and the nearest penultimate interglacial SLIP is located on the north Norfolk coast. Such limited information restricts the regional input to, and hence the relevance of, global reconstructions of late Middle and Late Pleistocene sea level. Marine-influenced deposits without such relevant data are known in Fenland, but their age and connection to past relative sea level (RSL) were largely uncertain. To improve this situation, new age-estimate data are presented and assessed in combination with existing age-estimate and new and existing palaeoecological data. Sea level relative to the marine-influenced deposits of Fenland is approximated based on brackish-marine faunal analyses. Results distinguish between marine-influenced deposits of penultimate and last interglacial sites. Fenland marine-influenced deposits of both interglacial stages share similar altitudinal envelopes (between a few metres above and below present ordnance datum (OD)), in common with Kirmington to the north and those of the British south coast, the Channel Islands and northwest France. Peak Fenland minimum RSL approximation (RSLA) of 2.5 m OD in the penultimate interglacial is commensurate with the north Norfolk coast SLIP but contrasts with the below OD peak of the global record. Timing of the peak Fenland maximum RSLA of 3.75 m OD late in the last interglacial at 116 ± 16 ka is commensurate with the Dutch record (116–105 ka), but contrasts with the early peak of some global records. © 2025 The Author(s). *Journal of Quaternary Science* Published by John Wiley & Sons Ltd.

KEYWORDS: amino-acid geochronolgy; Fenland, UK; luminescesce dating; marine isotope stages 7 and 5e; palaeoecology; palaeo-sea-level reconstruction

#### Introduction

Global sea level rose by 1.7 mm year<sup>-1</sup> between 1901 and 2010 (IPCC, 2013). For a number of reasons the rate of change varies spatially and temporally, but there is evidence of longterm acceleration of sea level rise (Horsburgh et al., 2020; and references therein). In the United Kingdom, the mean sea level has risen by 12-16 cm since 1900 (Marine Climate Change Impacts Partnership, undated), and at present is rising faster than the global average (National Oceanography Centre, 2025). With this ongoing threat of spatially and temporally variable higher sea levels, Pleistocene interglacial sea-level deposits, therefore, have the potential to provide valuable information to humankind as it seeks to mitigate the effects of anthropogenically induced climate change (IPCC, 2023). This is particularly so at higher latitudes (Dutton et al., 2015; Long et al., 2015) because they could provide insight into parameters of variables such as glacio-isostasy, magnitude and rates of relative sea-level change, and how these vary spatially and temporally.

\*Correspondence: H. E. Langford, as above. Email: h.langford@bbk.ac.uk

 $^\dagger \text{This}$  article is dedicated to John Whittaker who sadly died on 29 July 2023 as this article was being prepared.

Reconstructing palaeo-sea-level, however, is challenging because of limitations in (i) dating reliability and temporal and spatial representativeness of age-estimate data; (ii) determining actual sea level at a specific location (i.e., sea-level index points; SLIPs, Shennan, 1982) at a known point in time; (iii) determining local structural geology and glacio-isostatic history at glacial near and intermediate fields. Global palaeosea-level curves (including errors) are, therefore, associated with large uncertainties; for example, reconstructed penultimate interglacial global sea levels between ca. -30 and +15 m and last interglacial (LIG) sea levels between ca. -10 and +20 m (Bintanja et al., 2005; Bates et al., 2014; Grant et al., 2014; Spratt and Lisiecki, 2016). Quaternary climate chronology generally is based on orbital tuning of marine stratigraphic records tied to solar insolation at 65° N (Robinson et al., 2002), but differences in the tuning method used (Robinson et al., 2002) and spatial heterogeneity of the sediment record (Past Interglacials Group of PAGES, 2016) give rise to uncertainties in exact correlation at the global scale. Additionally, the increasing rarity of reliably dated SLIPS deeper in geological time makes direct age-control of such proxy records more difficult, thereby exacerbating the uncertainties in correlation (Dutton et al., 2009). At intermediateto near-field sites, glaciological processes increasingly govern

<sup>&</sup>lt;sup>1</sup>School of Social Sciences, Birkbeck University of London, London, UK

<sup>&</sup>lt;sup>2</sup>Department of Geography, University of Sheffield, Sheffield, UK

<sup>&</sup>lt;sup>3</sup>School of Geography, Queen Mary, University of London, London, UK

<sup>&</sup>lt;sup>4</sup>Department of Earth Sciences, The Natural History Museum, London, UK

<sup>&</sup>lt;sup>5</sup>Department of Geoscience, Aarhus University, Aarhus, Denmark

<sup>&</sup>lt;sup>6</sup>BioArCh, Department of Chemistry, University of York, York, UK

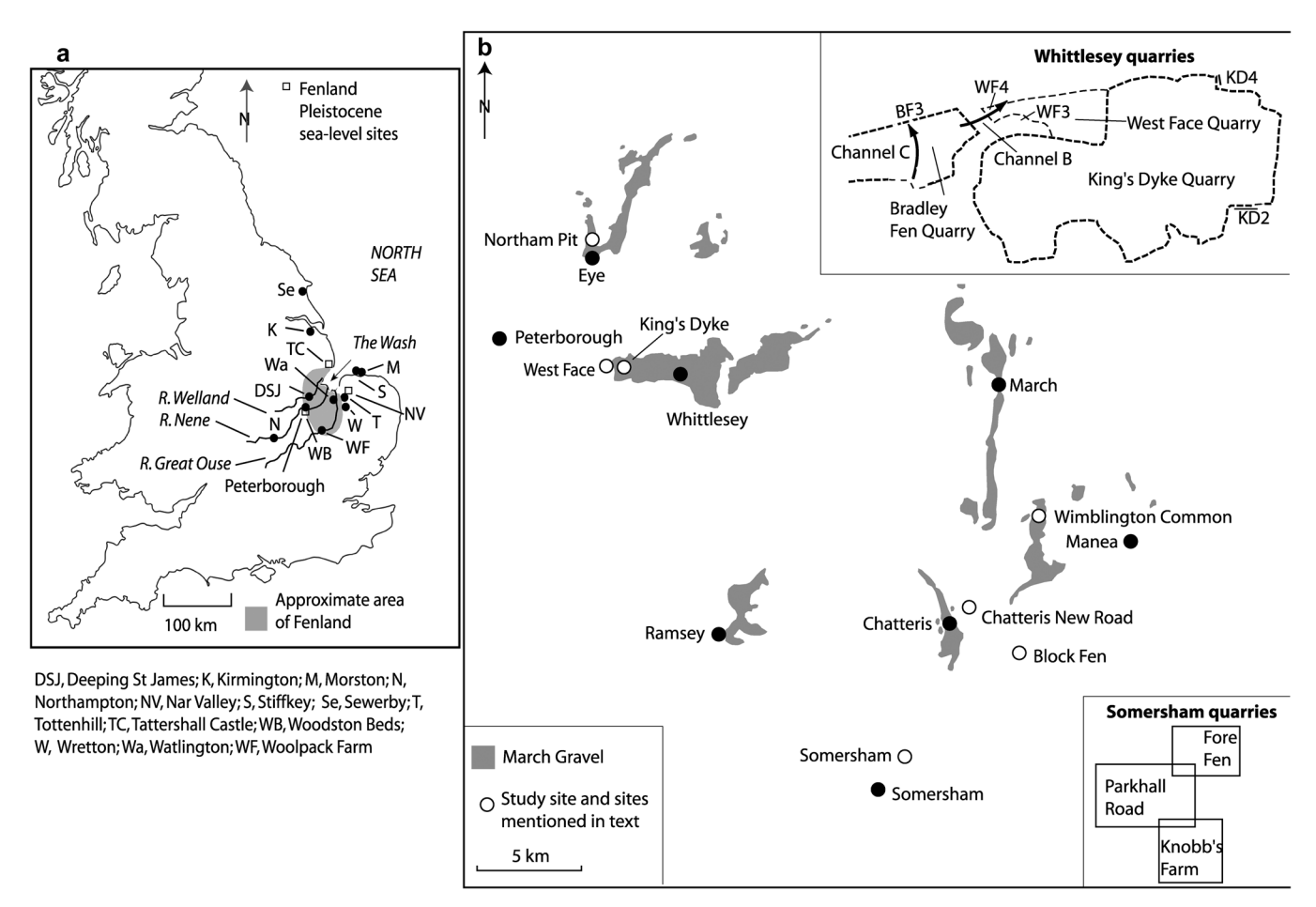


**Figure 1.** (a) Location of Fenland in eastern England and places mentioned in the text, including Fenland sea-level sites. (b) Distribution of March Gravel in western and central Fenland (BGS, 1980, 1984, 1995a, 1995b), with location of sections in the quarries at Whittlesey and at Somersham (West et al., 1999) shown as insets.

sedimentary factors on continental shelves and in marine basins (such as the North Sea) as ice builds and sea level falls, and under these circumstances, the preservation potential of SLIPs is extremely low. Increased direct age control and a more pragmatic approach to quantifying palaeo-sealevel data points (e.g., Cohen et al. (2022) also recognise reliably dated marine and terrestrial limiting SLIPs) could, therefore, reduce the uncertainties in global sea-level curves.

In Britain, there are few reported onshore and offshore sequences that record Pleistocene interglacial sea-level deposits, and this is particularly so for Fenland in eastern England (Fig. 1(a)). For example, the World Atlas of Last Interglacial Shorelines (WALIS) database (Cohen et al., 2022) records one SLIP in Fenland, that is, Tattershall Castle (Fig 1(a); Holyoak and Preece, 1985); the closest penultimate interglacial SLIP is located at Morston (Fig. 1(a)) on the north Norfolk coast. There are, however, several marine-influenced (i.e., presence of brackish-marine fauna) deposits recorded in Fenland (Sparks and West, 1970; Keen et al., 1990; Gao et al., 2000; West et al., 1994; West et al., 1995a, 1995b, 1999; Langford et al., 2004a) that could date to the penultimate or last interglacial, including the March Gravel (Baden-Powell, 1934). The aim of this study is to distinguish between penultimate and last interglacial marineinfluenced deposits in Fenland and determine where the relative sea level (RSL) lay at the time of deposition. New and existing data are utilised, mostly from sites where the geological, sedimentary and palaeoecology contexts have been published in detail (Table 1 and Fig. 2). As depicted in Fig. 2, only the marine-influenced elements and some

directly associated deposits of the relevant sequences are considered in this study.

Methods used to determine new infra-red stimulated luminescence (IRSL) data for feldspars from Northam Pit (Eye, Figs. 1(b) and 2), new amino-acid geochronology (AAG) data for Bithynia tentaculata opercula from Fore Fen (Somersham), West Face and King's Dyke (Whittlesey) quarries (Figs. 1(b) and 2), preliminary AAG data for foraminifera from Northam Pit and Fore Fen Quarry, as well as new palaeoecology data for Northam Pit and King's Dyke and West Face quarries are presented in order below. (Nomenclature for the guarries, sections and deposits has changed over the 30 years of investigation at Whittlesey. Langford et al. (2014b) provided details of those changes, and further details are included as Supplementary Material (Table S1).) Their corresponding results are presented in the following section. An important aspect of this study is the dual use of new and published age-estimate and fossilcontent data (Table 1) in order to establish reliably dated RSL approximations (RSLAs) in the Interpretation section. Another important aspect of the study is the inclusion of additional sites in the Discussion section in order to expand the number of RSLAs in Fenland. These fall into two categories: those that have reliably dated RSLAs (in addition to those in Fig. 2 and Table 1) and those that may have RSLAs but their age is uncertain. The discussion also considers stratigraphical grouping of Fenland RSLAs, implications for the marine-influenced March Gravel deposits, comparison with global records and proposed implications for Fenland evolution.

1/2025. See the Terms and Conditions (https://onlinelibrary.wiley.com/doi/01.0102/jqs.70025 by NICE, National Institute for Health and Care Excellence, Wiley Online Library for nules of use; OA articles are governed by the applicable Creative Commons Licenson

Table 1. Details of sites with new data for this study and with previously published data (Fig. 2).

			This stu	ıdy	Published		
Site name	Coordinates	Deposit*	Sample	Data	Reference	Data	
Northam Pit (NP; Eye)	0°112′ W,	March Gravel	Shfd19175	pIRSL	Keen et al. (1990): NP3 and NP4	М	
• •	52°369′ N		Shfd19183	pIRSL	2 m OD	Р	
			AAG-NP1	FAAG			
			AAG-NP2	FAAG			
			NP1 and 2	F, O			
WFQ (section WF3;	0°104′ W,	River Nene 1st Terrace	AAG-WF3	BAAG			
Whittlesey)	52°338′ N		AAG-U1	O			
			AAG-U2	O			
			Facies Sm	F, O			
KDQ (section KD4;	0°094′ W, 52°337′N	March Gravel	AAG-U3	O	Langford et al. (2004a):	$OSL^\dagger$	
Whittlesey)			Facies Fl	F, O	Shfd96130		
KDQ (section KD2;	0°095′ E, 52°338′ N	March Gravel	AAG-KD2	BAAG	Langford et al. (2004a): Shfd96131	$OSL^\dagger$	
Whittlesey)					Facies Fl-Fm/Sm	F, M, O	
FFQ (section SAO/SBK;	0°014′ E, 52°24′ N	River Great Ouse 2nd/	AAG-FF	BAAG	West et al. (1994, 1999):	F, M,	
Somersham)		1st Terrace		FAAG	Beds 2 and 3c	O, P	

BAAG, *Bithynia tentaculata* opercula amino acid geochronology; F, foraminifera; FAAG, foraminifera amino acid geochronology; FFQ, Fore Fen Quarry; IRSL, infra-red stimulated luminesce; KDQ, King's Dyke Quarry; M, molluscs; O, ostracods; OSL, optically stimulated luminescence measured on quartz at the single aliquot level using the Single Aliquot Regeneration method; P, pollen; WFQ, West Face Quarry.

#### Background

Fenland is a lowland area formed by accumulated late Middle to Late Pleistocene erosion of soft Upper Jurassic clays between consolidated Middle Jurassic limestones and Cretaceous Chalk, forming escarpments to the west and east, respectively; it is sometimes referred to as the Fen Basin but this could imply a structural geology feature (A. Pitty, personal communication, 1999) when that is not evident. Fenland is mostly situated on the East Anglia Massif segment of the London-Brabant Platform (LBP), which formed in the Permian Period (Fig. 3; Pharoah, 2018). In Cretaceous to Cenozoic times, the LBP experienced thermal subsidence. Although the effects of the Alpine orogeny on the LBP are largely unknown, except that to the east the Brabant Massif segment experienced subsidence in the North Sea, they appear to be coincident with the Variscan deformation front (Anderton et al., 1979). The northern margin of the LBP lies along the north Norfolk Coast and runs due west across The Wash into Lincolnshire, such that the northern edge of Fenland, including the Tattershall Castle (Fig. 1(a)) LIG site, is situated on the East Midland Shelf (EMS; Glennie, 1990). Undoubtedly, Fenland would have been affected by late Middle to Late Pleistocene glacioisostatic adjustment (GIA), but quantifying those effects in terms of MIS 7 and 5e sea-level histories at the local scale would be difficult because of uncertainties associated with ice limits (Langford, 2025). As far as we know, the effects of glacial overriding on the isostasy of the LBP have not been considered in modelled glacial or sea-level reconstructions. Modelling results to establish the maximum extent of the glacial forebulge warping associated with the Weichselian (Devensian) ice sheet suggest that Fenland could have experienced some upwarping (Busschers et al., 2007), which may also have been the case in marine isotope stages (MIS) 8 and 6 (Saalian; Fig. 3).

The most well-established Pleistocene interglacial sea-level deposits (those that record transgressive/regressive sequences) in Fenland are the Hoxnian (Holsteinian/MIS 11) sequences at Nar Valley (Fig. 1(a); Ventris, 1996) and Woodston (Fig. 1(a); Horton et al., 1992). West and co-workers have reported complex Ipswichian (Eemian/MIS 5e) marine-influenced deposits at Block Fen (Fig. 1(b); West et al., 1995a), Somersham (Fig. 1(b); West et al., 1999) and Wretton (Fig. 1(a); Sparks and

West, 1970). Stratigraphical assignment in these studies, however, has relied upon pollen biostratigraphy and, hence, there is the potential for conflation of more than one interglacial deposit (Thomas, 2001). Another widespread marine-influenced deposit is the March Gravel (Fig. 1(b); Baden-Powell, 1934), but its age and formation have been the subjects of debate (Skertchly, 1877; Marr and King, 1928; Turner, 1973; Castleden, 1980; Horton (in Douglas, 1981); West, 1987; Gallois, 1988, 1994; Horton, 1989; Bridgland et al., 1991; Langford, 1999; Langford and Briant, 2004; Boreham et al., 2010). Generally, the March Gravel has been regarded as the product of a single aggradation phase, but stratigraphical assignment has largely depended on altitude data and the presence of marine shells and microfauna. Caution is required, however, because, as demonstrated by West et al. (1994), there is the potential for reworking of such fauna from earlier deposits. Such is the status of the March Gravel that the exposure within it at Northam Pit (Fig. 1(b)) has been designated a geological Site of Special Scientific Interest (SSSI). In an investigation of the deposits at Northam Pit, Keen et al. (1990) concluded that the age was indeterminate based on the evidence then available.

#### **Methods**

#### Age-estimate analyses

#### Luminescence dating

Samples for luminescence dating from Northam Pit were originally collected in PVC tubes during site clearance of the SSSI section in 1999, but natural radiation could not be measured *in situ* at that time. In May 2019, after careful re-excavation, the original sample position of one of these (Shfd19183) was confirmed by relocating a black plastic bag deliberately left there. This enabled measurements to be made *in situ* using a sodium iodide EG&G Micronomad gamma spectrometer at the exact location of that sample, at about 2.5 m ordnance datum (OD), as well as at the location of a newly collected sample (Shfd19175) at about 2.4 m OD (Fig. 2).

<sup>\*</sup>Source: BGS, 1980, 1984, 1995b.

<sup>&</sup>lt;sup>†</sup> Details are provided as Supplementary Material (Tables S2–S4).

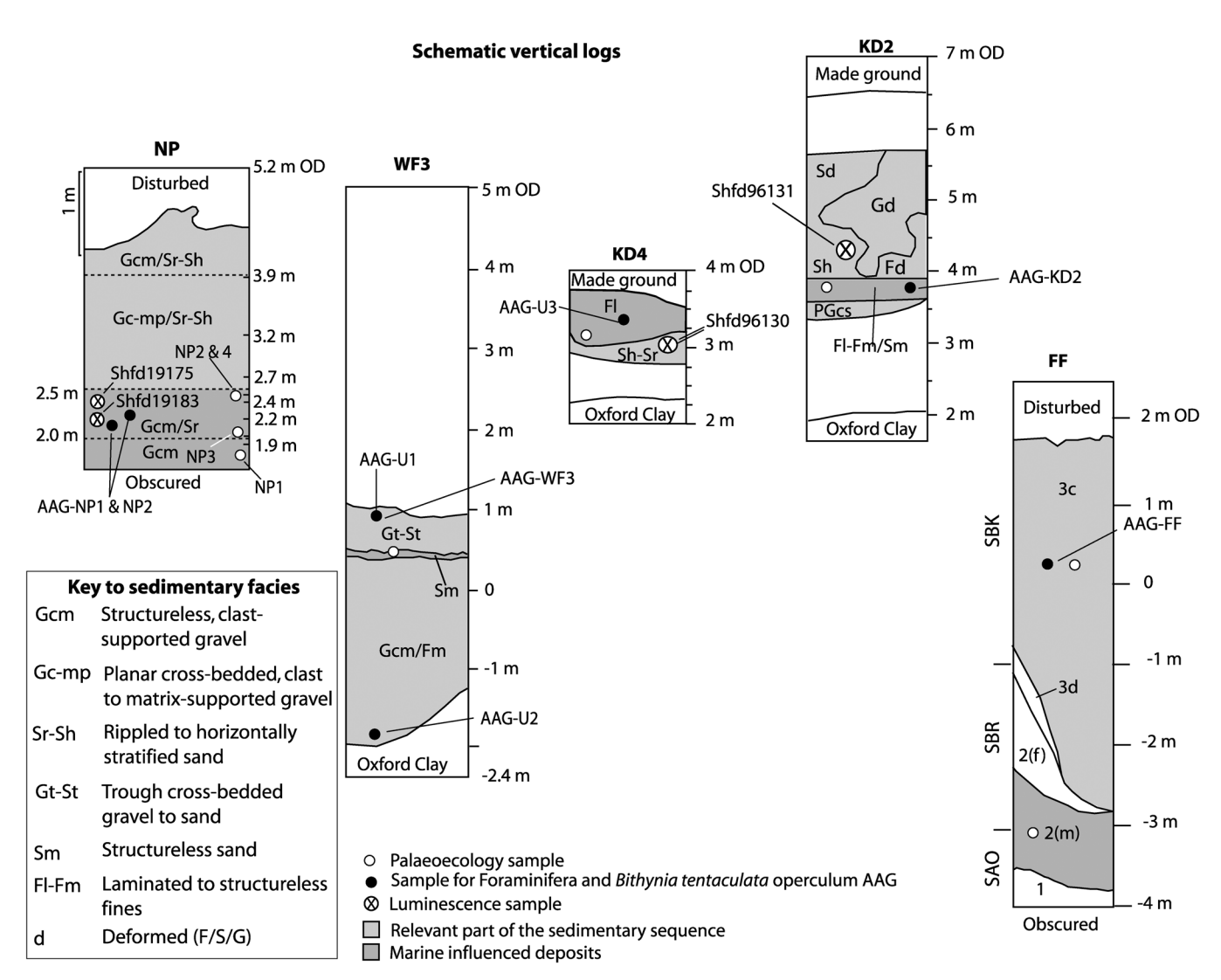


**Figure 2.** Schematic vertical logs of the sections studied at Northam Pit (NP), West Face (WF), King's Dyke (KD) and Fore Fen (FF) quarries. Relative locations of luminescence, palaeoecology, and AAG samples are shown. Palaeoecology samples are shown according to altitude on the NP log, but elsewhere a single datum represents that particular sedimentary facies at approximately that altitude. The sections are arranged according to surface elevation. Detailed elevation ticks on the NP log are referred to in the text. Facies nomenclature in log NP follows Bateman et al. (2020). Log FF is a composite of logs SBK/SBR/SAO from West et al. (1994), where bed nomenclature differs from that in West et al. (1999; 2 corresponds to D and 3c to H2), with (m) referring to marine and (f) to fluvial. AAG-U1-AAG-U3 refer to unsuccessful attempts at AAG dating of foraminifera (Appendix A).

Gamma spectrometer data were used to determine the gamma dose rate (Table 2). Bulk samples were analysed using inductively coupled plasma mass spectrometry (ICP-MS) to determine naturally occurring potassium (K), thorium (Th) and uranium (U), and these elemental concentrations were converted to beta dose rates using data from Guérin et al. (2011). An internal K content of 12% was assumed for the feldspar samples (Huntley and Baril, 1997). In all cases, dose-rate calculations took into account attenuation factors relating to sediment grain sizes used and density. Attenuation of dose by moisture used present-day moisture with a 5% error to incorporate fluctuations through time (Table 2). The contribution to dose rates from cosmic sources was calculated using the expression published in Prescott and Hutton (1994; Table 2).

For palaeodose  $(D_{\rm e})$  determination, the samples were prepared under subdued red lighting with extraction and cleaning of feldspar following the procedure outlined in Bateman and Catt (1996). For the small aliquot measurements, feldspar grains were mounted as a ca. 5 mm diameter monolayer on 9.6 mm diameter stainless steel discs. Each aliquot contained ca. 500 grains. An array of IR light-emitting diodes (LEDs) in a Riso automated luminescence reader (DA-20) provided the stimulation.

Given the potential late Middle Pleistocene age of the sediments at Northam Pit, IRSL dating of feldspar grains was chosen because the IRSL signal saturates more slowly and so older samples can be dated more reliably (Mahan and DeWitt, 2019). This study adopted post-50°C measurements at 225°C, that is, a pIRSL<sub>225</sub> protocol (Buylaert et al., 2012; Rhodes, 2015). This targets a relatively bleachable signal (compared with pIRIR<sub>290</sub>, for example) and also reduces any anomalous fading, as observed at lower temperatures by Spooner (1994) and Mahan and DeWitt (2019). Samples were analysed using the single aliquot regenerative (SAR) approach (Murray and Wintle, 2000, 2003), and up to seven regeneration points were used to characterise growth curves, with the first regeneration point being identical to the last to correct for sensitivity changes. Twenty-four aliquots of each sample were measured in an attempt to evaluate how reproducible  $D_{\rm e}$  results were and how well bleached the sediments may have been prior to burial. As Fig. 4 demonstrates, the  $D_{\rm e}$  distributions of three of the four measurements (Shfd19175 IRSL<sub>50</sub>, pIRSL<sub>225</sub> and Shfd19183 IRSL50) are broadly normally distributed and have overdispersion below 30% when outliers are removed. As a result, De values for age calculation purposes for these

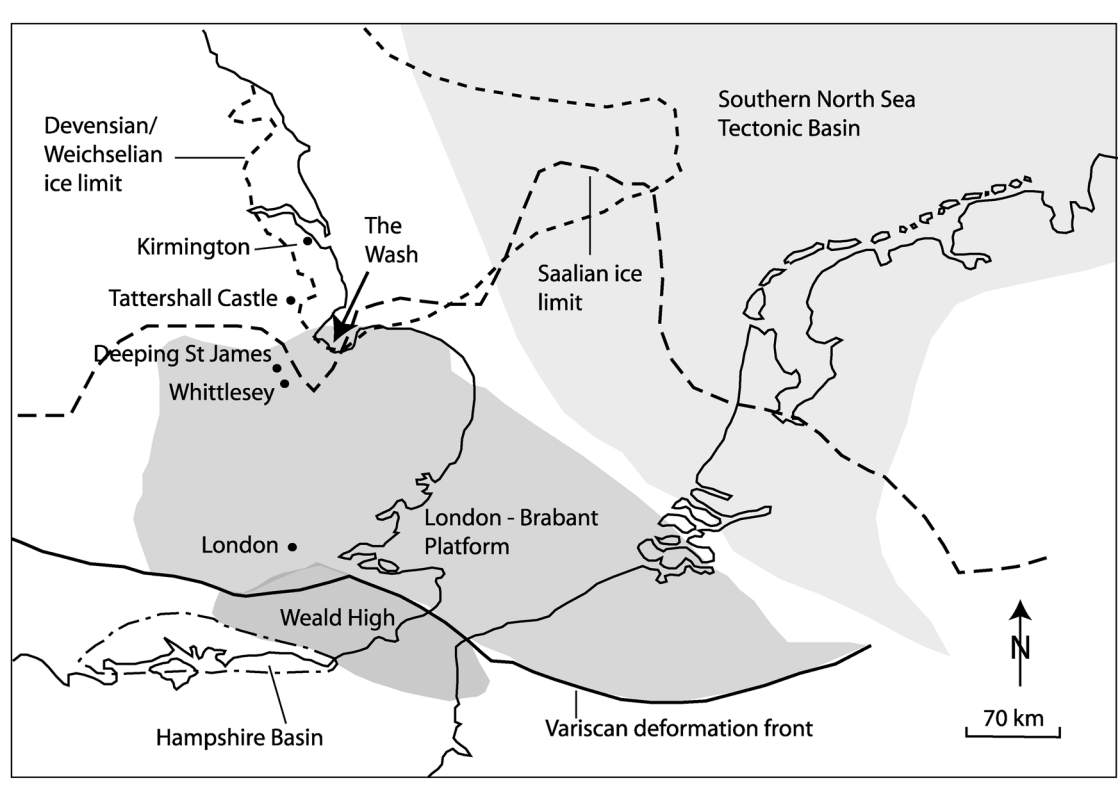


**Figure 3.** Tectonic features that could influence glacio-isostatic adjustment as well as accommodation space and preservation potential in the southern North Sea basin: London–Brabant Platform, Weald High and Variscan deformation front taken from Glennie (1990); Hampshire Basin approximated from Anderton et al. (1979); southern North Sea Tectonic Basin and Saalian (MIS 6) and Weichselian (MIS 5d–2) ice limits from Cohen et al. (2014).

Table 2. Summary of luminescence dosimetry related data for Northam Pit.

Data source	Laboratory code	Moisture (%)	U (ppm)	Th (ppm)	K (%)	D <sub>cosmic</sub> (Gy/ka)	Total dose rate* (Gy/ka)
Gamma spectrometer	Shfd19175	12 ± 5	_	_	_	$0.144 \pm 0.007$	2.111 ± 0.067
	Shfd19183	$12 \pm 5$	_	_		$0.146 \pm 0.007$	$2.155 \pm 0.089$
ICP-MS	Shfd19175	$12 \pm 5$	1.35	5.4	0.9	$0.144 \pm 0.007$	$2.324 \pm 0.073$
	Shfd19183	$12 \pm 5$	1.14	4.2	1.3	$0.146 \pm 0.007$	$2.368 \pm 0.094$
Combined <sup>†</sup>	Shfd19175	$12 \pm 5$	_	_		_	$2.125 \pm 0.081$
	Shfd19183	$12 \pm 5$	_	_	_	_	$2.170 \pm 0.097$

<sup>\*</sup>Total dose rate is attenuated for grain size, density and moisture.

measurements were extracted using the central age model (CAM) of Galbraith et al. (1999). In contrast, the pIRSL<sub>225</sub> De replicate results for sample Shfd19183 are skewed and multimodal with a high level of De replicate scatter (overdispersion > 30%), indicating that partial bleaching has influenced the harder to bleach pIRSL225 signal in this sample. Some aliquots for pIRSL<sub>225</sub> were saturated. As a result, De values for age calculation purposes were extracted using the finite mixture model (FMM) of Galbraith and Green (1990). The FMM calculated two components, of which the lowest (representing 86% of the data) is assumed to relate to the true burial age (Bateman et al., 2007). For the pIRSL<sub>225</sub>, a residual value of 10.7 Gy has been deducted from the final D<sub>e</sub> values based on measurements of prepared material exposed for over 1 week to Sheffield (United Kingdom) daylight. No fading correction was undertaken for the pIRSL<sub>225</sub> data as natural fading (not laboratory-induced fading) at elevated temperatures is reduced or not observable (e.g., Rhodes, 2015). In all cases, ages are quoted in years from the year of measurement and are presented with one sigma confidence intervals, which incorporate systematic uncertainties with the dosimetry data, uncertainties with the

palaeomoisture content and errors associated with the  $D_{\rm e}$  determination (Table 2).

#### Amino-acid geochronology of Bithynia tentaculata opercula

Two *B. tentaculata* opercula from King's Dyke (sample AAG-KD2), five from West Face (sample AAG-WF3) and five from Fore Fen (sample AAF-FF, Bed 3c) quarries (Fig. 2) were analysed for the determination of intracrystalline protein decomposition (IcPD). The *B. tentaculata* opercula were analysed by combining a reverse-phase high-pressure liquid chromatography (RP-HPLC) method of analysis (Kaufman and Manley, 1998) with the isolation of an 'intracrystalline' fraction of amino acids by bleach treatment (Sykes et al., 1995). This results in the analysis of the ratios of D- and L-forms (D/L) of multiple amino acids from the chemically protected (closed system) protein within the biomineral, which has been shown to increase the reliability of D/L determinations in *Bithynia* opercula (Penkman et al., 2011, 2013).

All samples were prepared using the procedures of Penkman et al. (2008b) to isolate the intracrystalline protein by bleaching with 12% NaOCl for 48 h. Two subsamples were

<sup>†</sup>Combined dose rate uses ICP-MS values for beta and alpha contributions and gamma spectrometer for gamma contributions.

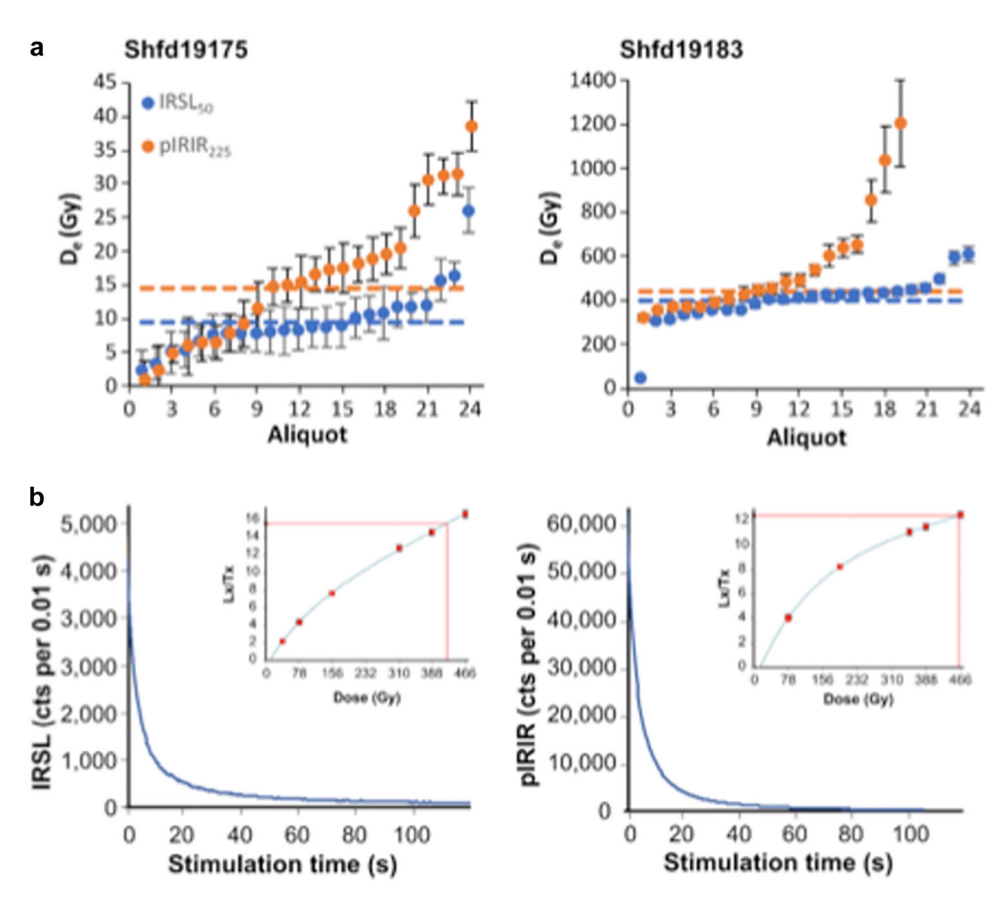


**Figure 4.** Luminescence data for the two samples from Northam Pit. (a)  $D_{\rm e}$  values as measured using IRSL<sub>50</sub> and pIRIR(IRSL)<sub>225</sub> with the extracted  $D_{\rm e}$  used in age calculation (see text for details) shown with the dashed lines. Note the low  $D_{\rm e}$  values for Shfd19175 taken to indicate recent light exposure during quarrying sufficient to partially reset both IRSL<sub>50</sub> and pIRSL<sub>225</sub> (although less so for the latter). For Shfd19183, note the better bleaching of the IRSL<sub>50</sub> data, but how  $D_{\rm e}$  extraction using FMM on the pIRSL<sub>225</sub> data returns a very similar result. (b) Shine-down curves and SAR growth curves for IRSL<sub>50</sub> (left) and pIRIR(IRSL)<sub>225</sub> (right) measurements. Note the rapid decay of the luminescence signal with stimulation time and the good fit of regenerative points to the SAR growth curve. [Color figure can be viewed at wileyonlinelibrary.com]

then taken from each operculum; one fraction was directly demineralised and the free amino acids analysed (referred to as the 'free' amino acids, FAA, F), and the second was treated to release the peptide-bound amino acids, thus yielding the 'total' hydrolysable amino acid fraction (THAA, H\*). Samples were analysed in duplicate by RP-HPLC, with standards and blanks run alongside samples. During preparative hydrolysis, both asparagine and glutamine undergo rapid irreversible deamination to aspartic acid and glutamic acid, respectively (Hill, 1965). It is, therefore, not possible to distinguish between the acidic amino acids and their derivatives, and they are reported together as Asx and Glx, respectively.

The D/L values of aspartic acid/asparagine, glutamic acid/glutamine, serine, alanine and valine (D/L Asx, Glx, Ser, Ala, Val) as well as the [Ser]/[Ala] value are then assessed to provide an overall estimate of IcPD. In a closed system, the amino acid ratios of the FAA and the THAA subsamples should be highly correlated, enabling the recognition of compromised samples (e.g., Preece and Penkman, 2005). The D/L of an amino acid will increase with increasing time, whereas the [Ser]/[Ala] value will decrease. Each amino acid racemises at different rates, and, therefore, is useful over different timescales. The D/L of Ser is less useful as a geochronological tool for samples of this age, but is presented here because aberrant values are useful indications of contamination.

#### Amino acid geochronology of foraminifera

Pilot AAG analyses were carried out on Ammonia spp. foraminifera from Northam Pit (samples AAG-NP1 and

AAG-NP2, facies Gcm/Sr; see Fig. 2 for key to sedimentary facies) and Fore Fen Quarry (sample AAG-FF, Bed 3c; Fig. 2). As experiments on various species of foraminifera, including Ammonia spp., have found limited improvements in intrasample variability when using the NaOCl procedure (Millman et al., 2022; Wheeler, 2022), a weak oxidative pretreatment (3% H<sub>2</sub>O<sub>2</sub> pretreatment for 2 h) was used in this study following the methods of Millman et al. (2022). In order to conserve material, only the THAA (H\*) fraction was analysed and analytical replicates were not carried out (Wheeler, 2022). Samples were analysed by RP-UHPLC using a method modified from Crisp (2013). The number of tests per replicate ranged from 23 to 55 (Table 4). Samples with [L-Ser]/[L-Asx] > 0.8, an indicator of modern contamination (Kosnik and Kaufman, 2008), were excluded from further analysis (Wheeler, 2022).

#### Sources and composition of faunal lists

For this study, samples from Northam Pit (NP1–NP4) and from King's Dyke (facies Fl, section KD4) and West Face (facies Sm, section WF3) quarries (Fig. 2) were processed for microfaunal analysis. Samples were prepared using standard techniques (e.g., Langford et al., 2014a). Brackish and marine habitat species lists for Northam Pit (for molluscs), King's Dyke (section KD2; foraminifera and ostracods) and Somersham (foraminifera, ostracods and molluscs) were augmented from the literature (Keen et al., 1990; Bridgland et al., 1991; West et al., 1994; West et al., 1999; Langford et al., 2004a). Additional lists of foraminifera supplied for unsuccessful AAG

dating (Wheeler, 2022, unpublished) at sections WF3 and KD4 were qualitatively assessed (Appendix A); ostracods picked at the same time were also identified and counted (Appendix B). Foraminiferal faunal lists compiled from marine-influenced sediments at Northam Pit, King's Dyke, West Face and Fore Fen quarries were compared with the habitat classifications of Jones and Whittaker (2010). Environmental preferences of marine and brackish water ostracods were based on Athersuch et al. (1989) and the literature cited therein.

#### Relative sea-level approximation determinants

Relative sea-level determinations for the study are based on faunal analyses of the fossil content of marine-influenced sediments in order to identify thanatocoenoses (autochthonous death assemblage—representative of an in situ life assemblage; Boomer et al., 2003), components of thanatocoenoses that have been transported largely intact from their natural depositional environment and taphocoenoses (allochthonous death assemblage; Boomer et al., 2003), indicative of postmortem transport and sorting. As the fossil assemblages studied do not contain biota sufficiently diagnostic to allow water depth to be determined, the pragmatic approach adopted here is to use what information is available to provide a meaningful estimate of RSL; using the qualifying terms brackish-estuarine limiting and fluvial limiting. In the context of this study, brackish-estuarine limiting is applied to deposits of an estuarine depositional system or deposits recording a fresh influx of brackish-estuarine fauna into a fluvial depositional system; fluvial limiting is applied to deposits of a fluvial depositional system or fresh influx of fluvial fauna into a brackish-estuarine depositional environment. As water depth cannot be determined, deposits of an estuarine depositional system are considered to provide minimum values; for fluvial deposits, it is assumed that the tidal limit lies downstream and therefore the RSLA is considered a maximum value. It should be emphasised here that previously published sedimentological or palaeoenvironmental interpretations have not been reviewed or reinterpreted as part of this study, and that the thickness of the marine-influenced sediments does not represent a range of estimated RSL.

#### Results

#### Luminescence

Sample Shfd19175 from Northam Pit was much younger than anticipated (Table 3), owing to reflection of past disturbance of the exposure face in 1999 (a strict sampling protocol, i.e., removing 50 cm of sediment from the face, could not be used for the collection of samples in 2019 because of the need to preserve the face intact as far as possible). Therefore, only the results for sample Shfd19183 are discussed here. Results for this sample gave an IRSL $_{50}$  age of  $182\pm10$  ka and a pIRSL $_{225}$  age of  $205\pm14$  ka (Table 3). As they are within errors of each other, it is reasonable to assume that the IRSL $_{50}$  age has not suffered

unduly from fading and that the sample was reasonably well bleached prior to burial (IRSL $_{50}$  more so as the pIRSL $_{225}$  required FMM to extract the resultant age). A combination of both measurements gives an age of  $194 \pm 17$  ka, equivalent to late MIS 7/early MIS 6 climatic stages.

## Amino acid geochronology of Bithynia tentaculata opercula

The FAA versus THAA Ala D/L covariance for the 12 *B. tentaculata* opercula analysed (five from AAG-FF, five from AAG-WF3 and two from AAG-KD2) are plotted in Fig. 5 against the UK aminostratigraphic framework, with previously published results for Fore Fen Quarry highlighted (Penkman et al., 2011, 2013). These plots indicate an age equivalent to MIS 7 for facies Gt–St at section WF3 and a maximum MIS 7 age for facies Fl–Fm/Sm at section KD2 and Bed 3c at section SBK (because their fossil assemblages are taphocoenoses; see later). The IcPD data for the 12 *B. tentaculata* opercula analysed are available as Supplementary Material (Table S5).

#### Pilot amino acid geochronology of foraminifera

Data for Asx D/L and Glx D/L are presented in Table 4 and plotted in Fig. 6. Only the THAA fraction was analysed due to limited material, but the relationship between Asx D/L and Glx D/L for the samples was found to be consistent with closed-system behaviour (Penkman et al., 2008b). While the comparative foraminifera framework is limited, with no data from other UK Pleistocene sites confidently assigned to MIS 7 (Wheeler, 2022), the Northam Pit and Fore Fen Quarry foraminifera have D/L values at the upper end of the range of sites assigned to MIS 7-5e, and are lower than independently dated English Pleistocene sites assigned to MIS 9 or older. This is consistent with the IRSL date from Northam Pit (Shfd19183, Table 3) and the opercula AAG dating from Fore Fen Quarry (AAG-FF, Fig. 5), corroborating a MIS 7 attribution for facies Gcm/Sr at Northam Pit and a maximum MIS 7 age for Bed 3c at Fore Fen Quarry.

## Palaeoecological contribution to the determination of RSLAs

As it is not possible to establish SLIPs at any of the study sites, faunal analysis of brackish-marine Foraminifera, Ostracoda and Mollusca assemblages formed the basis for the determination of brackish-estuarine limiting RSLAs. Table 5 details faunal lists of brackish and marine palaeoenvironmental indicator species for the study sites. Additional species identified in the material supplied for unsuccessful AAG dating of foraminifera (Appendix A) in facies Gt–St and Fl at sections WF3 and KD4, respectively, have been added to Table 5 as appropriate. Qualitative assessment of the species lists for these two facies indicates that they are not in conflict with the interpreted depositional environment of the marine microfauna. For economy of space, some of the rare occurrences of foraminifera species recorded

Table 3. Summary of single aliquot palaeodose data and derived ages.

Laboratory code	Depth (m)	Protocol	D <sub>e</sub> (Gy)	OD* (%)	Dose rate (Gy/ka)	Age (ka)
Shfd19175	2.8	IRSL <sub>50</sub> pIRSL <sub>225</sub>	$9.58 \pm 0.68$ $7.0 \pm 2.72$	31 (0) 33 (31)	$2.125 \pm 0.081$	$4.51 \pm 0.36$ $3.28 \pm 1.30$
Shfd19183	2.7	IRSL <sub>50</sub> pIRSL <sub>225</sub>	$395 \pm 11$ $445 \pm 23$	47 (11) 39 (23)	$2.170 \pm 0.097$	$182 \pm 10$ $205 \pm 14$

<sup>\*</sup>Values in parentheses are after outliers and saturated aliquots have been removed.

(West et al. 1994, 1999) and Langford et al. (2004a) are not listed. Included in Table 5(a) are habitat classifications for Foraminifera (Jones and Whittaker, 2010).

At 1.9 m OD (sample NP1, Table 5(a)) in the Northam Pit sequence (facies Gcm, Fig. 2), the foraminifera faunal assemblage of nine species includes an estuarine to shallow marine fauna dominated by a superabundance of *Ammonia batavus* (large/ornate) together with an abundance of *Haynesina germanica* and *Elphidium clavatum* and *Elphidium* 

selseyensis. Note that taxon *E. clavatum/E. selseyensis* includes both the 'cold/northern' species *E. clavatum* (i.e., those presently occurring at more northern latitudes) and the boreal species *E. selseyensis* (cf. Darling et al., 2016). These two species have not been counted separately in the present work. Marine specimens, however, dominate, with a superabundance of *Elphidium macellum* together with an abundance of *Cibicides lobatulus*. The presence of proximal marine conditions is also supported by the relatively rich marine assemblage

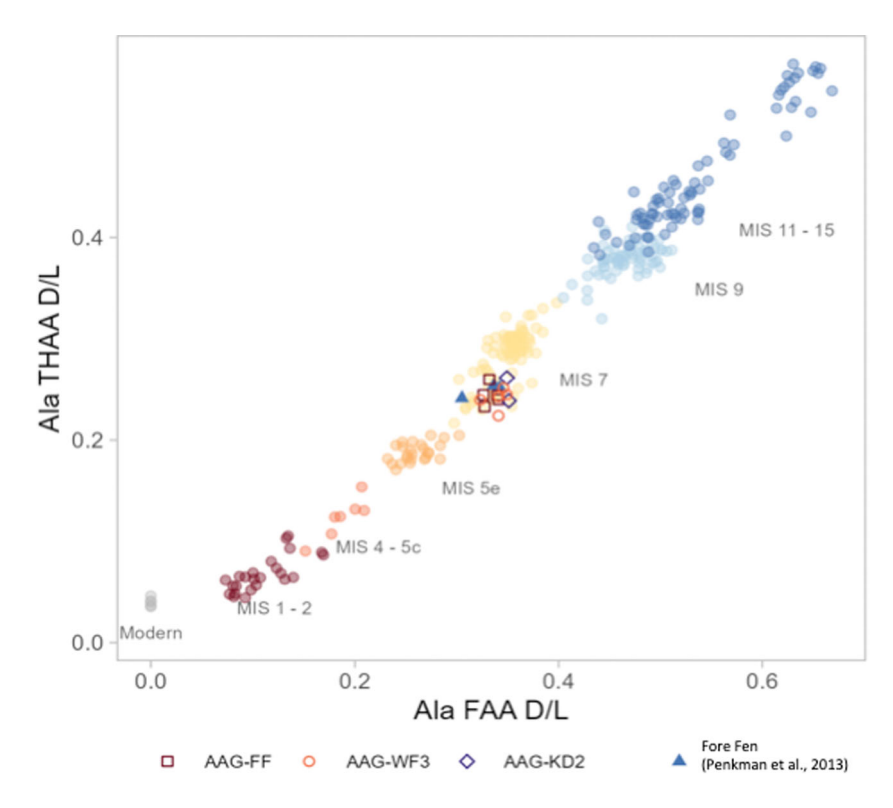


**Figure 5.** The Ala FAA D/L versus THAA D/L data for two *B. tentaculata* opercula from facies FI–Fm at section KD2 (sample AAG-KD2, Fig. 2), King's Dyke Quarry (Whittlesey), for five *B. tentaculata* opercula from Bed 3c of section SBK (sample AAG-FF, Fig. 2) at Fore Fen Quarry (Somersham) and for five *B. tentaculata* opercula from facies Gt–St of section WF3 (sample AAG-WF3), West Face Quarry (Whittlesey), compared with the UK *B. tentaculata* opercula AAG framework (Penkman et al., 2011), 2013). Previously published opercula AAG results from Fore Fen Quarry (Penkman et al., 2013) are shown for comparison. [Color figure can be viewed at wileyonlinelibrary.com]

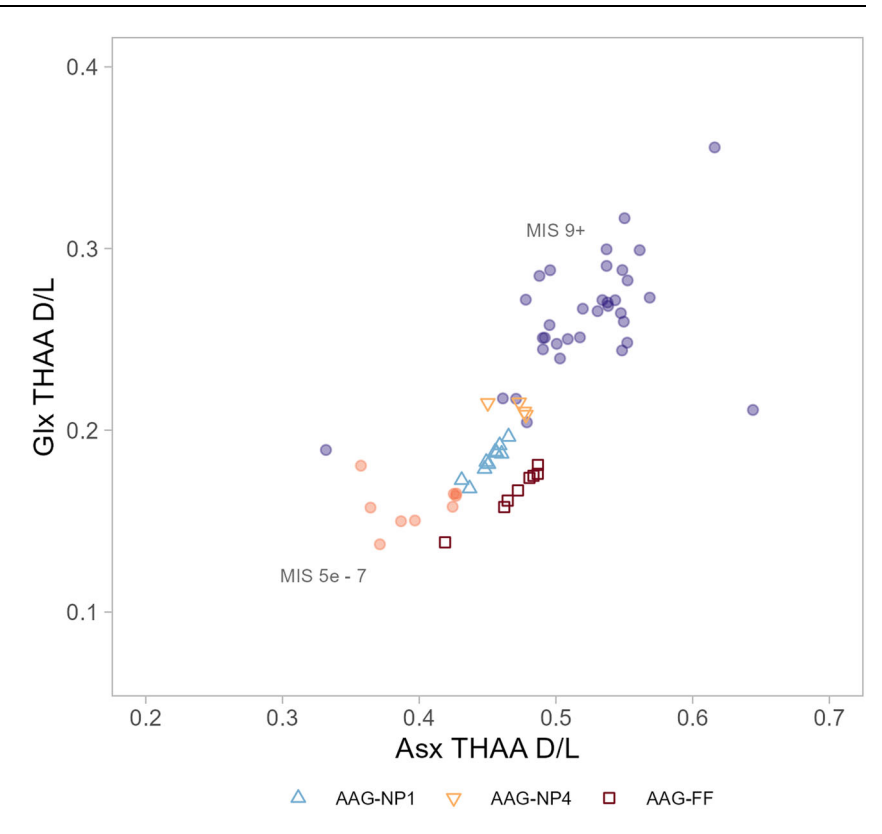
**Table 4.** Average THAA Asx and Glx D/L values for *Ammonia* spp. foraminifera from Northam Pit, Eye and Fore Fen Quarry, Somersham (Figs. 1(b) and 2).

Sample <sup>†</sup>	Neaar number/sample code	Species	Number of tests	Asx d/l	Glx d/l	[L-Ser]/[L-Asx]
AAG-NP1	AB149-3x2hH*	Ammonia spp.	50	0.43	0.17	0.30
	AB150-3x2hH*	Ammonia spp.	50	0.46	0.19	0.23
	AB151-3x2hH*	Ammonia spp.	50	0.45	0.18	0.31
	AB152-3x2hH*	Ammonia spp.	50	0.45	0.18	0.25
	AB153-3x2hH*	Ammonia spp.	50	0.46	0.19	0.26
	AB154-3x2hH*	Ammonia spp.	50	0.44	0.17	0.32
	AB155-3x2hH*	Ammonia spp.	50	0.47	0.20	0.22
	AB156-3x2hH*	Ammonia spp.	50	0.45	0.18	0.25
	AB157-3x2hH*	Ammonia spp.	50	0.46	0.19	0.22
	AB158-3x2hH*	Ammonia spp.	50	0.46	0.19	0.23
AAG-NP2	13606bH*	Ammonia spp.	30	0.45	0.21	0.58
	13607bH*	Ammonia spp.	30	0.48	0.21	0.56
	13608bH*	Ammonia spp.	30	0.47	0.22	0.76
	13609bH*	Ammonia spp.	23	0.48	0.21	0.51
AAG-FF	13390bH*	Ammonia spp.	45	0.36	0.12	$0.97^{\ddagger}$
	13391bH*	Ammonia spp.	45	0.33	0.10	1.16 <sup>‡</sup>
	13392bH*	Ammonia spp.	45	0.32	0.09	1.29 <sup>‡</sup>
	17254bH*	Ammonia spp.	50	0.46	0.16	0.48
	17255bH*	Ammonia spp.	55	0.48	0.18	0.30
	17256bH*	Ammonia spp.	55	0.46	0.16	0.31
	17257bH*	Ammonia spp.	55	0.47	0.17	0.25
	17258bH*	Ammonia spp.	55	0.49	0.18	0.28
	17259bH*	Ammonia spp.	55	0.48	0.17	0.34
	17260bH*	Ammonia spp.	55	0.49	0.18	0.22
	17261bH*	Ammonia spp.	55	0.42	0.14	0.42

<sup>&</sup>lt;sup>†</sup>AAG-NP1 and AAG-NP2, facies Gcm/Sr, Northam Pit, Eye; AAG-FF, Bed 3c, section SBK, Fore Fen Quarry, Somersham.

<sup>\*</sup>Samples excluded from further analysis due to [L-Ser]/[L-Asx] > 0.8, indicative of modern contamination.

**Figure 6.** The Asx versus Glx THAA D/L values for *Ammonia* spp. from Northam Pit, Eye and Fore Fen Quarry, Somersham (Figs. 1(b), 2), overlaid on other foraminifera D/L values from independently dated English Pleistocene deposits (Wheeler, 2022). Samples with [L-Asx]/[L-Ser] values > 0.8 have been excluded from the figure to show variability of D/L values in foraminifera. Samples AAG-NP1 and AAG-NP4 are from facies Gcm/Sr at Northam Pit, and AAG-FF is from Bed 3c, section SBK, Fore Fen Ouarry.



of ostracods at 1.9 m OD (sample NP1, Table 5(b)), dominated by Hemicythere villosa and Cythere lutea. Of the 'cold/ northern' climatic indicators, only Buccella frigida is present amongst the foraminifera. 'Cold/northern' indicator species Sarsicytheridea bradii and Hemicytherura clathrata are common, and Finmarchinella angulata is present amongst the ostracods. It should be noted that the 'cold/northern' indicator species listed in Table 5(a) and (b) commonly occur in interglacial assemblages. The assemblage of marine molluscs (sample NP3, Table 5(c)) at 2 m OD, particularly the abundance of *Pholas dactylus* (Keen et al., 1990), also suggests proximal marine conditions. Chenopodiaceae in the pollen assemblage from a mud clast in gravel at this level indicates marine-brackish conditions, with Carpinus also present, indicating late temperate conditions (Keen et al., 1990). At 2.2 m OD (facies Gcm/Sr, Fig. 2) a foraminiferal assemblage of nine species with a superabundance of H. germanica and A. batavus and an abundance of Elphidium williamsoni indicates a change to low-salinity estuarine conditions (Keen et al., 1990). No 'cold/northern' indicator species were recorded in this assemblage. This change to more estuarine conditions is also reflected in the nine species of foraminifera present at 2.5 m OD, including the appearance of Elphidium waddense (sample NP2, Table 5(a)). The warm-water species Aubignyna perlucida (Whittaker et al., 2005; Jones and Whittaker, 2010) is also common at this level, whereas there is an absence of 'cold/northern' indicator species. Freshwater ostracods (seven species, with three representing cool climate conditions—not reported here) also make their first appearance at this level, presumably introduced to the estuary by riverine transport. Cyprideis torosa is superabundant here and at 1.9 m OD, and is smooth rather than noded, suggesting that salinity was not too low (in contrast to the view of Keen et al., 1990), and the presence of juvenile instars at both levels suggests that this represents a living assemblage, a feature also noted by Keen et al. (1990). The number of 'cold/northern' marine species increases from three to five, with F. angulata, Palmenella limicola and Robertsonites tuberculatus being common and S. bradii and Elofsonella concinna being present. The restricted

mollusc assemblage at this level (Keen et al., 1990), comprising brackish *Hydrobia* species, also testifies a change to a more estuarine environment (sample NP4, Table 5(c)).

A sequence of three samples (unpublished) at Northam Pit from 2.7 to 3.9 m OD (facies Gc-mp/Sr-Sh, Fig. 2) comprised foraminifera of the four species most abundant in facies Gcm and Gcm/Sr (*A. batavus, E. macellum, H. germanica, E. williamsoni*), frequently with a rolled, polished and chipped appearance. Likewise, the ostracods were restricted in numbers between two and five species, mostly represented by broken valves of *C. torosa*.

Marine-influenced sediments are present in the fully temperate mixed-oak woodland to late temperate woodland sediments of Bed 2(m) at section SAO at Fore Fen Quarry, Somersham (Fig. 2; West et al., 1994), where they cropped out at about -3.7 to -3.0 m OD and were sampled at about -3.3 m OD. The foraminifera fauna is dominated by the superabundance of estuarine-intertidal species *E. clavatum/E. selseyensis* and *H. germanica* and the abundance of *Ammonia batavus* and *Elphidium gunteri*; the ostracod fauna by the superabundance of *C. torosa* and *Loxoconcha elliptica*; and the mollusc fauna by the superabundance of *H. ventrosa* and the abundance of *H. ulvae*. 'Cold/northern' indicator species *B. frigida* and *C. reniforme* are present amongst the foraminifera, but there are none present amongst the ostracods (Table 5(a) and (b)).

Section SBK at Fore Fen Quarry cropped out from at least –1 to a minimum of 1.7 m OD (Bed 3c, Fig. 2; West et al., 1994; West et al., 1999), with sampling carried out between 0 and 1 m OD, including that used for the opercula AAG dating and *Ammonia* spp. of foraminifera (sample AAG-FF, Figs. 2, 5 and 6). The fossil assemblage includes 'cold/northern' indicators *B. frigida* and *C. reniforme* amongst the foraminifera, and all but *Semicytherura similis* and *P. limicola* amongst the ostracods (Table 5(b)).

The earliest appearance so far of foraminifera (*E. williamsoni* and *H. germanica*) in the MIS 7 sequence at West Face Quarry was recorded from a sample for molluscan analysis (unpublished) at about –2 m OD at the base of facies Gcm/Fm in section WF3 (Fig. 2), along with the earliest record so far of the marine/outer

1099147, 0, Downloaded from https://onlinelibrary.wiley.com/do/10.1002/jas.70025 by NCE, National Institute for Health and Care Excellence, Wiley Online Library on [171112025]. See the Terms and Conditions (https://onlinelibrary.wiley.com/terms-and-conditions) on Wiley Online Library for rules of use; OA articles are governed by the applicable Creative Commons License

**Table 5.** Brackish and marine palaeoenvironmental indicator species recorded for this study (samples NP1 and NP2 and sections KD4 and WF3) and reported in the literature (sections KD2, SBK and SAO).

(a) Habitat classifications (columns 2–6) of Jones and Whittaker (2010) and semiquantitative counts of foraminifera (columns 7–14)

	Н	abitat c	lassif	ication	ns								
	S	S							KD:	2			
Species	High	Low	H/I	L/O	S/M	NP1	NP2	KD4	Fl–Fm	Sm	WF3	SBK	SAO
Entzia (=Jadammina) macrasens (Brady, 1870)													
Miliammina fusca (Brady, 1870)													
Trochammina inflata (Montagu, 1808)													
Ammonia aberdoveyensis (Haynes, 1973)*		+				C	C	Α			Α		
Ammonia parkinsoniana (d'Orbigny, 1839)		+											
Elphidium clavatum Cushman, 1930/Elphidium selseyensis (Heron-Allen & Earland, 1911)		+				Α	С	(A)	SA	С	Α	SA	SA
Elphidium williamsoni (Haynes, 1973)*		+				C	SA	Α	C	C	Α	C	C
Haynesina germanica (Ehrenberg, 1840)*		+				Α	SA	SA	Α	C	SA	SA	SA
Aubignyna perlucida (Heron-Allen & Earland, 1913) <sup>‡</sup>							C				(C)	R	
Ammonia batavus (Hofker, 1951)*			+			SA	SA		C	Р	P <sup>dwarfed</sup>	SA	Α
Ammonia flevensis (Hofker, 1930)			+										
Elphidium earlandi (Cushman, 1936)			+										
Elphidium gerthi van (Voorthuysen, 1957)			+			C			C				R
Elphidium magellanicum (Heron-Allen & Earland, 1932)			+					(P)	C	Р	(P)	R	C
Haynesina depressula (Walker & Jacob, 1798)			+					(P)			(p)	C	C
Cibicides lobatulus (Walker & Jacob, 1798)				+		Α	C	(C)	SA	C		Α	
Elphidium incertum (Williamson, 1858)				+				(C)				C	
Elphidium waddense (van Voorthuysen, 1951)				+			C				Р		
Stainforthia fusiformis (Williamson, 1858)				+				(P)	R	SA	Р		
Elphidium macellum (Fichtel & Moll, 1798)						SA	Α		R		Р	Р	
Buccella frigida (Cushman, 1922)						Р			C	Р	Р	Р	R
Buccella frigida calida (Cushman & Cole, 1930)								(C)			(P)		C
Trifarina angulosa (Williamson, 1858)								Р			Р	Р	
Cassidulina reniforme (Nørvang, 1945)									C	Р	Р	Р	R
Elphidium albiumbilicatum (Weiss, 1954)								(C)	C	Р	(C)	C	Р
Elphidium margaritaceum (Cushman, 1930)									R	R	Р	R	
Cassidulina laevigata (d'Orbigny, 1826)									R	C		R	
Epistominella vitrea (Parker, 1953)										C			
Hyalinea baltica (Schroeter, 1783)										C			
Nonionella turgida (Williamson, 1858)										C			
Pullenia osloensis (Feyling-Hanssen, 1954)									R	C			
Haynesina orbiculare (Brady, 1881)									R	R		C	
Elphidium gunteri (Cole, 1931)											(C)		Α

#### (b) Ostracoda

					KD	2			
Habitat	Species	NP1	NP2	KD4	Fl–Fm	Sm	WF3	SBK	SAO
Brackish	Cyprideis torosa (Jones, 1850)	SA <sup>S</sup>	SA <sup>S</sup>	P <sup>S</sup>			Cs	SA	SA
	Cytheromorpha fuscata (Brady)	Р	C				C	Р	
	Loxoconcha elliptica (Brady, 1868)	С	Р				Р	Α	SA
	Leptocythere psammophila (Guillaume, 1976)						C		
	Leptocythere lacertosa (Hirschmann, 1912)						C		
	Leptocythere castanea (Sars, 1866)						Р		C
	Leptocythere porcellanea (Brady, 1869)						Р		C
Marine	Hirschmannia viridis (O.F. Müller, 1785)*				Р		Р		
	Hemicythere villosa (Sars, 1866)	Α	C		Р		Р	Α	
	Cythere lutea (O.F. Müller,1785)	C	С		Р		Р	SA	Р
	Eucythere argus (Sars, 1866)	Р	Р				Р	Р	
	Leptocythere pellucida (Baird, 1850)						Р		
	Palmoconcha laevata (Norman, 1865)						Р		
	Semicytherura undata (Sars, 1866)						Р	Р	
	Semicytherura nigrescens (Baird, 1838)		C		Р	Р	Р	Р	C
	Semicythere sella (Sars, 1866)	Р					Р		C
	Semicytherura similis (Sars, 1866)				Р	Р	Р		
	Robertsonites tuberculatus (Sars, 1866)		C				Р	C	
	Hemicytherura cellulosa (Norman, 1865)				Р		Р	Р	C
	Hemicytherura clathrata (Sars, 1866)	C					Р	Α	
	Finmarchinella angulata (Sars, 1866)	Р	C				Р	C	
	·							(Ca	ontinued)

17/11/2025, See the Terms and Conditions (https://oinleibbary.wiley.com/doi/01.0102/js;70025 by NCE, National Institute for Health and Care Excellence, Wiley Online Library or [17/11/2025]. See the Terms and Conditions (https://onlineibbary.wiley.com/terms-and-conditions) on Wiley Online Library for rules of use; OA articles are governed by the applicable Creative Commons License

 Table 5. (Continued)

/I \	$\sim$ .			- 1	
(h)	Ost	rac	$^{\circ}$	n:	,

		KD2								
Habitat	Species	NP1	NP2	KD4	Fl–Fm	Sm	WF3	SBK	SAO	
	Finmarchinella finmarchica (Sars, 1866)*				Р		Р	А		
	Cytheropteron latissimum (Norman, 1865)	C	Р					Α		
	Cuneocythere semipunctata (Brady, 1868)						Р			
	Sarsicytheridea bradii (Norman, 1865)	C	Р					Р		
	Palmenella limicola (Norman, 1865)		C							
	Elofsonella concinna (Norman, 1865)		С					Р		

(c) Mollusca

				S	m
Habitat	Species	NP3	NP4	KD2	SAO
Brackish	Hydrobia ventrosa		Р		SA
	(Montagu) agg				
	Hydrobia ulvae (Pennant)		Р		Α
	Mercuria confusa (Frauenfeld)				Р
Marine	Littorina littorea (Linné)	Р		Р	
	Turritella communis Risso	Р			
	<i>Mytulis edulis</i> Linné	С			
	Ostrea edulis Linné	С			
	Cerastoderma edule Linné	С	Р		Р
	Spisula solida (Linné)	Р			
	<i>Macoma balthica</i> (Linné)	Р			
	Scrobicularia plana (da Costa)	С			
	Pholas dacylus Linné	A			

Greyshade denotes species characteristic of that classification, and crosses denote species that may be found in that classification: SS, supratidal saltmarsh; H/I, high intertidal/inner estuarine; L/O, low intertidal/outer estuarine; S/M, subtidal/marine.

NP, Northam Pit. Counts by J. Whittaker April 2008: superabundant (SA)  $\geq$  50; abundant (A) 11–49; common (C) 2–10; present (P) 1; NP1, 1.9 m OD: NP2, 2.5 m OD.

KD, King's Dyke. Section KD4 personal assessment by J. Whittaker, February 2016; entries in parentheses are additions from Appendix A. Section KD2 counts converted to percentages by K. L. Knudsen 1999: SA,  $\geq$ 20%; A, 10%–19%; C, 2%–9%; P, 1%–2%; rare (R), <1%.

WF, West Face. Section WF3 personal assessment by J. Whittaker 2004; entries in parentheses are additions from Appendix A.

Sections SBK and SAO at Somersham reported by West et al. (1994): SA, ≥20%; A, 10%–19%; C, 2%–9%; P, 1%–2%; rare (R), <1%.

‡Present in facies PGcs at KD2. **Bold** typeface indicates species with cold/northern affinities.

NP3, 2 m OD; NP4, 2.5 m OD.

estuarine ostracod Hemicythere villosa and the brackishpsammophila; estuarine species Leptocythere brackish-estuarine ostracod species C. torosa (smooth) and Cytheromorpha fuscata also occurred but these species had been previously recorded in the earlier MIS 7 channel B sediments (Langford et al., 2014a); subsequent investigation proved this molluscan sampled sediment to be far richer in marine microfauna than previously thought (Appendices A and B). A significant influx of brackish-marine microfauna was recorded at about 0.40-0.45 m OD in section WF3, where a medium-fine sand ribbon (Sm, Fig. 2; comprising mostly microfauna) no more than 5 cm thick yielded a superabundance of microfossils, including echinoid spines and the common presence of freshwater molluscs, some with well-preserved striations (Fig. 7(a), (b)). The foraminifera fauna is dominated by the abundance to superabundance of estuarine-intertidal species A. aberdoveyensis, E. clavatum/E. selseyensis, E. williamsoni and H. germanica, with A. batavus also being present. Several subtidal-marine species are present, but numbers are low. As with the foraminifera, brackishestuarine species (C. torosa (smooth), C. fuscata, L. psammophila and Leptocythere lacertosa) dominate the ostracod fauna and

several marine species are present, but again numbers are low. Amongst the foraminifera, the 'cold/northern' indicator species *B. frigida*, *E. clavatum* and *C. reniforme* are present. Dwarfed *A. batavus*, in response to a cooler climate, is also present. Note, however, that a 'cold/northern' aspect is not evident in the counts of Appendix A. Six out of nine of the 'cold/northern' indicator ostracod species are also present.

A small sample (<50 g) of fine silt (~150 µm) from facies Fl at section KD4 (Fig. 2) at about 3 m OD in King's Dyke Quarry proved to be rich in foraminifera, with estuarine–intertidal species *H. germanica* being superabundant and *Ammonia* aberdoveyensis, *E. clavatum/E. selseyensis* and *E. williamsoni* abundant (Table 5(a)). Outer estuarine–open marine species *Cibicides lobatulus, Trifarina angulosa* and small specimens of *Elphidium* spp., as well as lagenids and bolivinids, were present in limited numbers. A limited fresh and brackish water ostracod fauna comprised mostly juveniles and included *C. torosa*. No climatic indicator species were present amongst either the foraminifera or ostracods.

Fossiliferous deposits (facies PGcs, Fl–Fm/Sm, Sh and Fd) were recorded between 3.3 m and about 5.7 m OD at section

<sup>\*</sup>Listed in Keen et al. (1990) along with Elphidium articulatum (d'Orbigny), Elphidium crispum (Linné) and Guttelina problema (d'Orbigny), samples at about 2.2 m OD.

ŚSmooth.

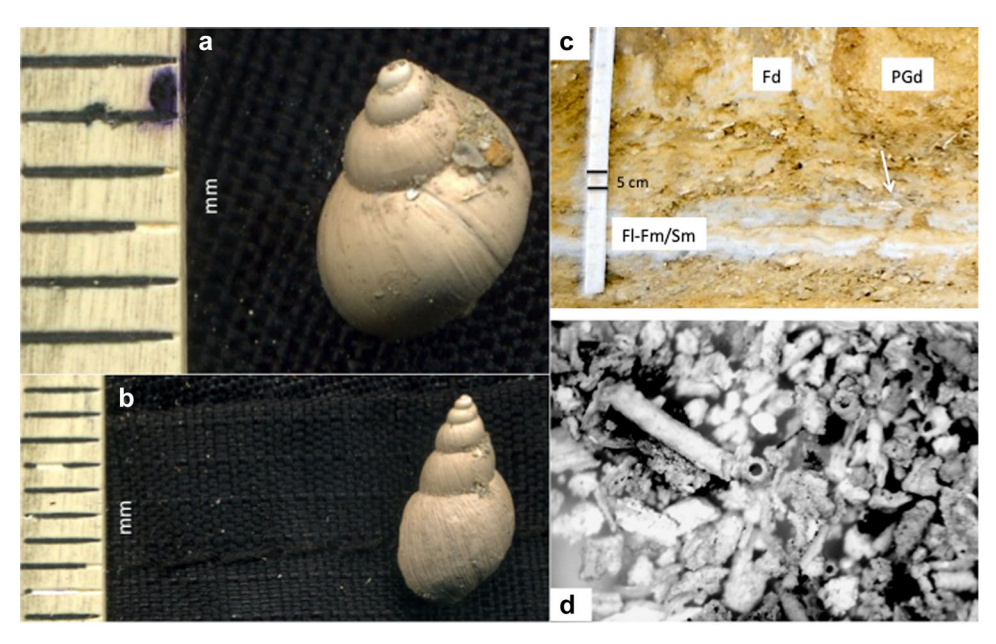


**Figure 7.** Freshwater gastropods in facies Sm of section WF3 (West Face Quarry, Whittlesey) with well-preserved striations: (a) *Bithynia tentaculata*; (b) *Galba truncatula*. Species identification by Tom Meijer. (c) Facies Fl–Fm/Sm at section KD2 and (d) *Chara* tubes from the Sm component. The arrow in (c) indicates a bisected articulated unionid bivalve (probably *Anodonta* sp. given the depositional environment; Killeen et al., 2004) about 5 cm long, suggesting stability of the substrate for at least 4 years (Aldridge, 1999). [Color figure can be viewed at wileyonlinelibrary.com]

KD2 in King's Dyke Quarry (Fig. 2). A diverse fauna of 58 foraminifera has been recorded at the species level (Langford, 1999; Langford et al., 2004a) from these four facies. As the AAG dating of B. tentaculata opercula reported here are from facies Fl-Fm/Sm (3.7-3.9 m, Fig. 2), Table 5(a) lists some of the 26 foraminifera identified to species level in the Fl-Fm (laminated to structureless silt) component and the 25 in one of the sand ribbons represented by facies Sm. Facies FL-Fm/Sm (Fig. 7(c)) accumulated in a shallow, clear, highly calcareous freshwater pool in which Chara (Fig. 7(d)) grew profusely, as evidenced from an abundance of both oospores and tubes (Langford, 1999). Eleven species of foraminifera are common to all four fossiliferous facies: E. clavatum/E. selseyensis, E. williamsoni, H. germanica, Elphidium gerthi, Elphidium magellanicum, C. lobatulus, E. macellum, B. frigida, A. batavus and C. reniforme. Therefore, a wide range of habitats is represented, from inner estuarine to subtidal. The only noticeable difference between the samples from facies FL-Fm/ Sm as a whole (as well as among all four facies investigated) and the particular sand ribbon sampled separately is that the latter has reduced numbers or none at all (E. gerthi and E. macellum) of these species. Nine species of the overall faunal list are unique to the sand ribbon (e.g., Epistominella vitrea, Hyalinea baltica, Nonionella turgida; Table 5(a)) and the species composition indicates relatively deep water (subtidal to middle shelf), particularly characterised by the superabundance of Stainforthia fusiformis. Almost all species recorded for this sand ribbon are interglacial in character, whereas all other counts commonly include the 'cold/northern' indicator species indicated in Table 5(a). In addition, the concentration of benthic foraminifera in this sand ribbon is 12 times that in the laminated to structureless silt, the number of planktonic specimens is 27 times that in the laminated to structureless silt, and specimens in this sand ribbon tend to be well preserved whereas in all other facies most specimens are whitish with a chemically etched surface and evidence of mechanical abrasion is common (Langford, 1999; Langford et al., 2004a). The ostracod and molluscan faunal assemblages recorded for facies PGcs, FI-Fm/Sm, Sh and Fd overwhelmingly indicate a freshwater habitat, supported by the sedimentology, and pollen analyses

indicate cold conditions for facies Fd (Langford, 1999; Langford et al., 2004a). Although nine marine ostracod species are recorded, they are represented by a total count of 31 abraded juvenile valves for all four facies, consistent with possible reworking from older deposits. The 'cold/northern' indicator species *S. similis* is present in both the laminated to structureless silt and the sand ribbon, whereas *Finmarchinella finmarchica* is present only in the laminated to structureless silt. The presence of *Heterocypris salina* and *Candona angulata* could indicate mildly saline inner estuarine conditions, but both species can also inhabit non-saline environments.

#### Interpretation

#### Northam Pit

It is evident that the samples at 1.9 m OD and at 2.5 m OD are thanatocoenoses from an estuarine river mouth setting (category B of Cohen et al., 2022) that consequently correlate, or closely correspond, with the age of deposition. These thanatocoenoses therefore provide a brackish-estuarine limiting minimum RSLA of 2.5 m OD for the Northam Pit sequence, and the assumed riverine influx of freshwater ostracods provides a fluvial limiting minimum RSLA at 2.5 m OD (NP, Fig. 8(a)). The IRSL age determined on feldspars from sample Shfd19183 (Table 2), ranging from  $182 \pm 10 \text{ ka}$  (IRSL<sub>50</sub>) to  $205 \pm 14 \text{ ka}$  (pIRSL<sub>225</sub>), with a combined age of  $194 \pm 17$  ka, places the estuarine conditions of facies Gcm/Sr, and hence the late temperate woodland minimum RSLA of 2.5 m, at the end of MIS 7 (Fig. 9(a)). More specifically, the median pIRSL225 age plots within MIS 7c and at one sigma confidence interval appears to provide a maximum age of MIS 7c. The median combined age corresponds to MIS 7a, but its one sigma confidence interval spans from the MIS 7c-b transition to MIS 6. Consequently, which of these climate substages the minimum RSLA of 2.5 m should be assigned to remains tentative. Preliminary AAG dating of Ammonia spp. of foraminifera from facies Gcm/Sr at Northam Pit supports an age equivalent to MIS 7 (Fig. 6) for the estuarine-marine microfauna, which could rule out the possibility of reworking of older fossil microfauna.

1/11/12025. See the Terms and Conditions (https://onlinelibrary.wiley.com/toi/i0/10/10/2/js, 70025 by NICE, National Institute for Health and Care Excelence, Wiley Online Library for nules of use; OA articles are governed by the applicable Creative Commons, the policy of the terms and Conditions (https://onlinelibrary.wiley.com/terms-a-d-conditions) on Wiley Online Library for nules of use; OA articles are governed by the applicable Creative Commons, and Conditions (https://onlinelibrary.wiley.com/terms-a-d-conditions) on Wiley Online Library for nules of use; OA articles are governed by the applicable Creative Commons, and Conditions (https://onlinelibrary.wiley.com/terms-a-d-conditions) on Wiley Online Library for nules of use; OA articles are governed by the applicable Creative Commons, and Conditions (https://onlinelibrary.wiley.com/terms-a-d-conditions) on Wiley Online Library for nules of use; OA articles are governed by the applicable Creative Commons, and Conditions (https://onlinelibrary.wiley.com/terms-a-d-conditions) on Wiley Online Library for nules of use; OA articles are governed by the applicable Creative Commons, and Conditions (https://onlinelibrary.wiley.com/terms-a-d-conditions) on Wiley Online Library for nules of use; OA articles are governed by the applicable Creative Commons, and the common of the comm

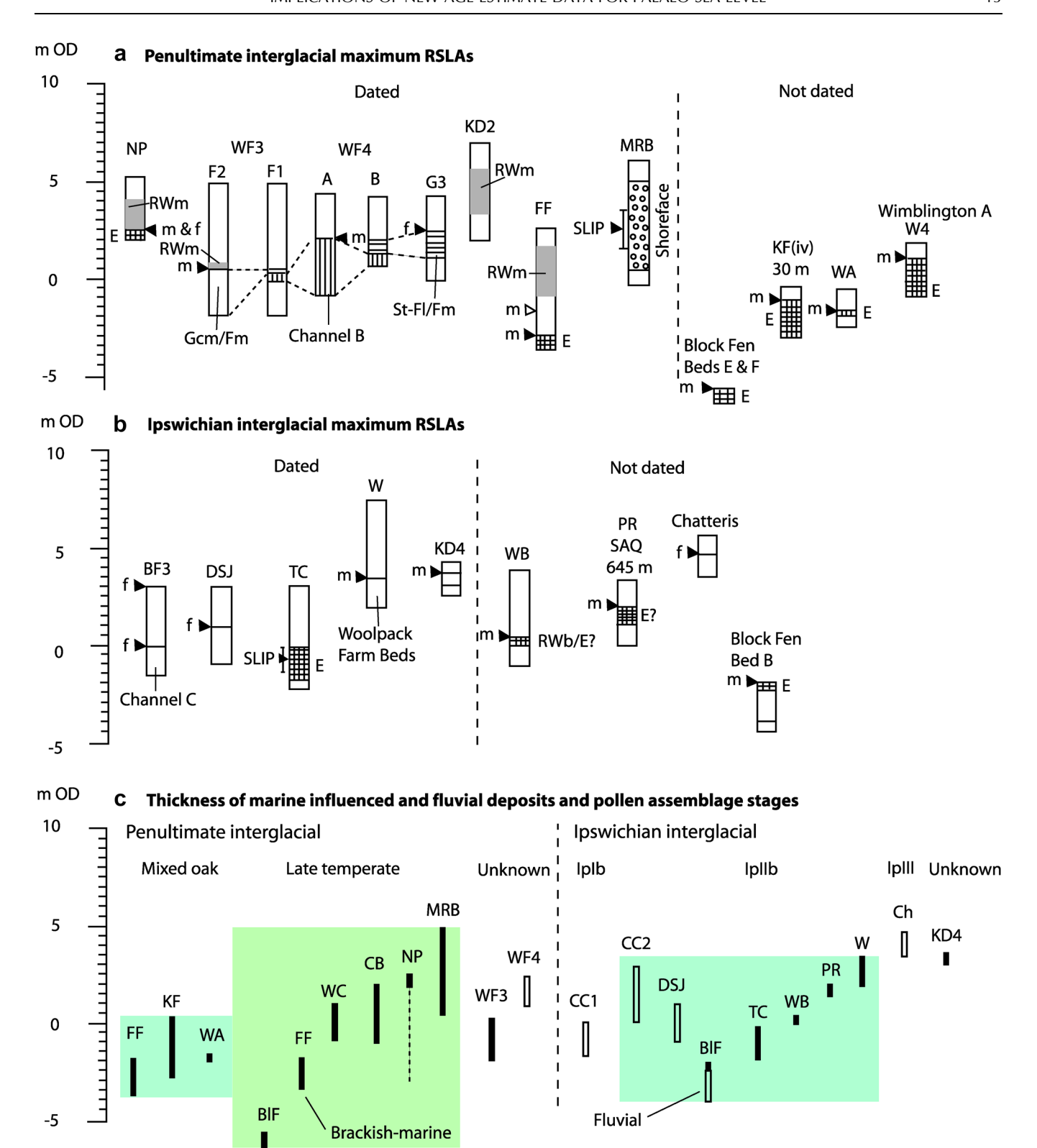


**Figure 8.** (a) Fenland penultimate interglacial maximum RSLAs and Morston raised beach SLIP plotted against altitude: m, brackish—marine limiting; f, fluvial limiting. The upper RSLA on the FF log represents that for Fore Fen Quarry, whereas the lower represents that at section SAO. Logs F1 and B have been included to show the stratigraphical relationship of channel B, facies St–FI/Fm and facies Gcm/Sm at West Face Quarry. (b) Fenland lpswichian maximum RSLAs and Tattershall Castle SLIP plotted against altitude. The two RSLAs on log BF3 represent last interglacial (LIG) pollen stages lp1b and lpIlb. Sites to the right of the vertical dashed lines may include RSLAs based on their fossil assemblages, but they are not dated reliably. E, brackish—marine; RWb, reworked brackish; RWm, reworked brackish—marine; NP, Northam Pit; WF, West Face; KD, King's Dyke; FF, Fore Fen; KF, Knobb's Farm; WA, WB, sites A and B at Wretton; MRB, Morston raised beach; BF, Bradley Fen; DSJ, Deeping St James; TC, Tattershall Castle; PR, Parkhall Road; W, Woolpack Farm; '?' denotes uncertainty in the cited sources of the depositional environment interpreted. (c) Thickness of marine-influenced and fluvial deposits identified as recording RSLAs arranged according to pollen assemblage stages where known. For the Fore Fen and Knobb's Farm quarries, the altitudinal ranges are combinations for that quarry reported in West et al. (1999). The dashed line at NP indicates the recorded thickness of March Gravel (Booth, 1982). BIF, Block Fen; WC, Wimblington Common; CB, channel B; WF3, facies Gcm/Fm; WF4, facies St-Fl/Fm; CC, channel C; Ch, Chatteris. [Color figure can be viewed at wileyonlinelibrary.com]

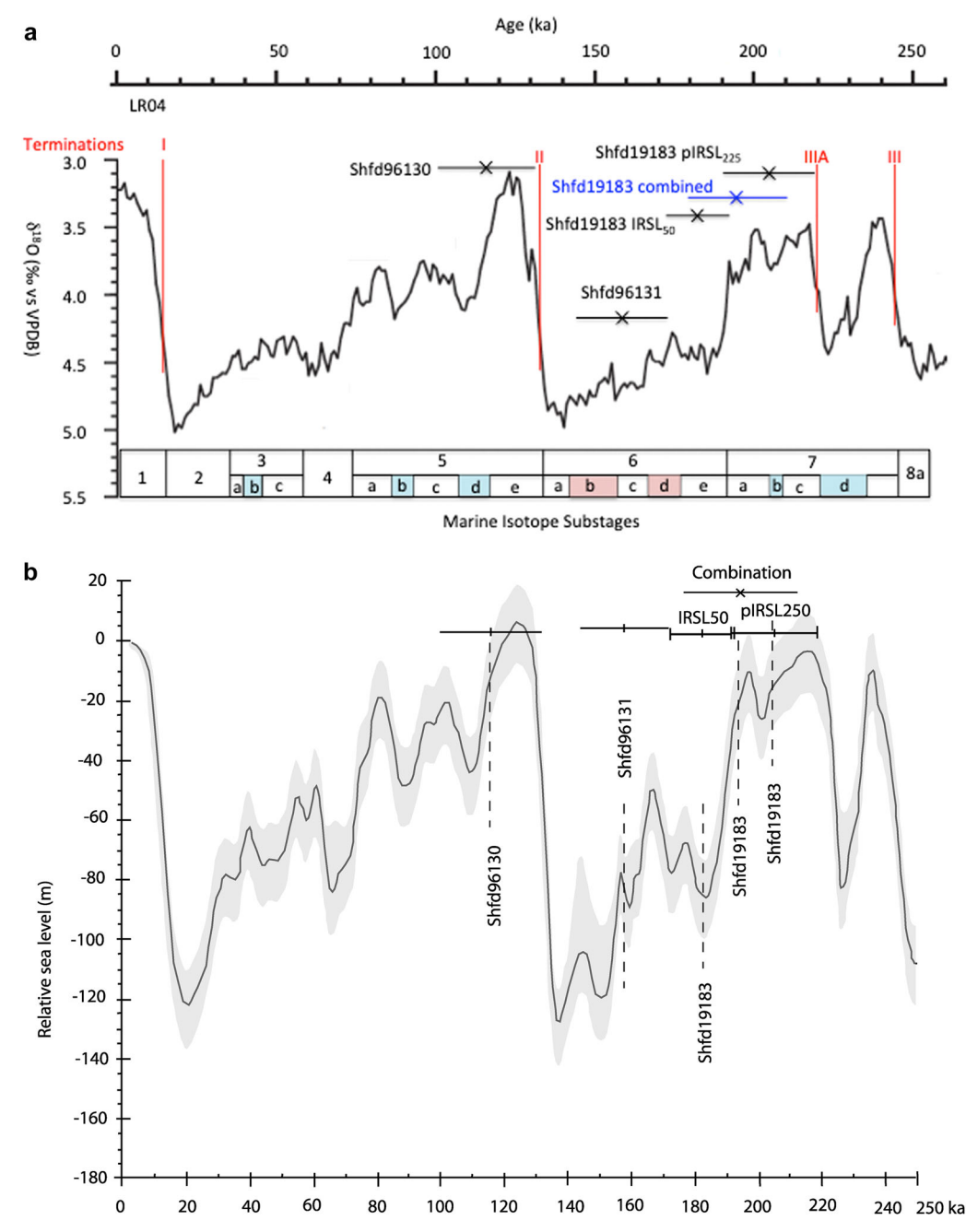


**Figure 9.** (a) Luminescence dates from Northam Pit (Shfd19183) and King's Dyke Quarry (Shfd96130 and Shfd96131) plotted against the LR04 stacked benthic  $\delta^{18}$ O records of Lisiecki and Raymo (2005) and the lettered marine isotope substages scheme of Railsback et al. (2015). (b) Luminescence dates from Northam Pit and King's Dyke Quarry plotted against a global RSL curve for the past 250 ka, with confidence interval shaded (Waelbroeck et al., 2002; after Antonioli, 2012). [Color figure can be viewed at wileyonlinelibrary.com]

The data from 2.7 to 3.9 m OD suggest that the fauna of facies Gc-mp/Sr-Sh is a taphocoenosis, including the most diverse molluscan assemblage reported by Keen et al. (1990) at 3.2 m OD, and hence not suitable for establishing a RSLA (RWm at NP, Fig. 6(a)). As the contact between facies Gc-mp/Sr-Sh and underlying facies Gcm/Sr is erosional, the former would not necessarily be fluvial limiting within the same regressional sequence.

#### Fore Fen Quarry

According to West et al. (1994) this biocoenosis assemblage (actually a thanatocoenosis; a biocoenosis is an assemblage of living organisms and the term is not applicable to fossils; see Boomer et al., 2003) from Bed 2(m) at section SAO represents temperate brackish conditions and provides a minimum

brackish–estuarine limiting RSLA of  $-3.0\,\mathrm{m}$  OD (lower m at FF, Fig. 8(a)); the molluscan element especially indicates an extreme inner estuarine river mouth setting. In West et al. (1999), however, marine-influenced sediments of Bed D (the equivalent of Bed 2) cropped out between -3.7 and  $-1.7\,\mathrm{m}$  OD, thereby suggesting a minimum brackish–estuarine limiting RSLA of  $-1.7\,\mathrm{m}$  OD (upper m at FF), but this is not supported by faunal analyses of sediments at these other sites in Fore Fen Quarry.

West et al. (1994) noted that the fossil assemblage of Bed 3c is markedly different from that of underlying Bed 2(m), and concluded that it was clearly a reworked 'thanatocoenosis' (actually a taphocoenosis; see Boomer et al., 2003) given the variety of habitats represented, with the possibility that different aged deposits were being reworked (RWm at FF, Fig. 8(a)). As the contact between Bed 3 and underlying Bed 2

17/11/2025, See the Terms and Conditions (https://oinleibbary.wiley.com/doi/01.0102/js;70025 by NCE, National Institute for Health and Care Excellence, Wiley Online Library or [17/11/2025]. See the Terms and Conditions (https://onlineibbary.wiley.com/terms-and-conditions) on Wiley Online Library for rules of use; OA articles are governed by the applicable Creative Commons License

is erosional, the former would not necessarily succeed fluvial limiting Bed 2(f) within the same regressional sequence.

Opercula AAG dating (sample AAG-FF, Figs. 2 and 5) provides a maximum MIS 7 age for Bed 3c of section SBK. As the fauna form a taphocoenosis, it is not feasible to provide a RSLA. Preliminary AAG dating of Ammonia spp. of foraminifera from Bed 3c supports an age equivalent to MIS 7 (Fig. 6) for the estuarine-marine microfauna, and potentially provides a minimum MIS 7 age for Bed 2(m) and a probable lower bracketing age of MIS 6 for the reworking. Although an age equivalent to MIS 7 for accumulation of the underlying marine-influenced sediments at section SAO also could be implied, as the marine-brackish fauna of SBK is distinct from that of SAO, an older age is possible. The fossil assemblage of Bed 2(m) at section SAO, especially the molluscan element (West et al., 1994), therefore, provides a brackish-estuarine limiting minimum RSLA of -3 m OD with a minimum age of MIS 7.

#### West Face Quarry

Although there is no direct supporting molluscan evidence, the fossil assemblage of facies Sm at section WF3 strongly suggests accumulation of contemporary estuarine to intertidal faunas and deposition by a tidal/storm surge rather than reworking of pre-existing sediments (i.e., both foraminifera and ostracods form estuarine to intertidal thanatocoenoses); it is considered that size sorting in this depositional process has precluded a brackish molluscan element from this assemblage. Facies Sm, therefore, provides a brackishestuarine limiting RSLA of 0.45 m OD (F2, Fig. 8(a)). Facies Sm has not been dated directly but the opercula AAG dating (AAG-WF3, Fig. 5) from facies Gt-St provides an upper bracketing age of MIS 7; a lower bracketing age of MIS 7 is provided by opercula AAG dating from channel B (Fig. 1(b) inset and A, B and F1, Fig. 8(a); Langford et al., 2007, 2014a), which is cut out by underlying facies Gcm/Fm (Fig. 2). Thus, an age equivalent to MIS 7 can be assigned to the brackishestuarine limiting maximum RSLA of 0.45 m for the sequence Gcm/Fm-Sm.

#### King's Dyke Quarry

As the species compositions of the ostracod and molluscan assemblages of facies PGcs and Fl-Fm/Sm at section KD2 do not fit easily into a particular palaeoenvironmental scenario, the possibility must be considered that at least some components of these assemblages are derived from older deposits. Although the origin of the sampled sand ribbon in facies FI-Fm/Sm remains enigmatic, the foregoing considerations suggest a taphocoenosis for facies PGcs and Fl-Fm/Sm (RWm at KD2, Fig. 8(a)). The AAG dating of B. tentaculata opercula (AAG-KD2, Figs. 2 and 5) provides a maximum MIS 7 age for facies Fl-Fm/Sm. Thus, the AAG dating and an upper bracketing OSL age of  $158 \pm 14$  ka for overlying facies Sh (Figs. 2 and 9(a); Langford et al., 2004a) indicate an age equivalent to MIS 7 for facies Fl-Fm/Sm and underlying PGcs. As the fossil fauna appears to form a taphocoenosis, it is not feasible to provide a RSLA.

The foraminifera of facies FI at section KD4 form an estuarine to intertidal thanatocoenosis, but the ostracod evidence is not sufficiently strong to arrive at the same conclusion. Nevertheless, facies FI is also interpreted as a tidal/storm surge deposit upstream of the tidal limit, with size sorting a major characteristic in its assemblage, and it provides a maximum brackish–estuarine limiting RSLA of  $3.75 \, \mathrm{m}$  OD (KD4, Fig. 8(b)). An OSL date of  $116 \pm 16 \, \mathrm{ka}$  on a

sand lens (Shfd96130, Fig. 2; Langford et al., 2004a) provides an underlying bracketing age for facies Fl. A minimum bracketing age is provided by extensive cryogenic deformation of section KD4 (Langford et al., 2004a), which also occurs at section WF3, where OSL data provide a maximum age of MIS 5a (Langford et al., 2007). The median OSL date of 116 ka plots on the MIS 5e–d transition and at one sigma confidence interval spans MIS 5e–c of the  $\delta^{18}O$  records of Fig. 9(a). The thanatocoenosis characteristics of the foraminifera fauna from facies Fl imply correlation with deposition and hence can be no older than the lower bracketing age of MIS 5e. Facies Fl, therefore, provides a brackish–estuarine limiting maximum RSLA at 3.75 m OD at the end of MIS 5e.

#### **Discussion**

#### Extension of RSLAs to other Fenland sites

Identification of RSLAs at other well-dated Fenland sites (Fig. 1) relies upon published interpretations of relevant data at West Face Quarry (Langford et al., 2007, 2014a), Bradley Fen Quarry (Langford et al., 2017), Deeping St James (Keen et al., 1999), Tattershall Castle (Holyoak and Preece, 1985) and Woolpack Farm (Gao et al., 2000), as well as the MIS 7 SLIP at Morston on the north Norfolk coast (Hoare et al., 2009; WALIS\_ID RSL\_4063, Cohen et al., 2022) and other publications cited below.

The late temperate woodland shoreface deposit (0.43 to  $5.03\,\mathrm{m}$  OD) at Morston (MRB, Fig. 8(a)) records a SLIP at  $2.5\pm1\,\mathrm{m}$  OD and between 1.9 and 2.9 m OD is dated by OSL on quartz grains to  $180\pm19$  (SA-MORST-1),  $184\pm21$  (SA-MORST-2) and  $191\pm19\,\mathrm{ka}$  (SA-MORST-4). Facies St–FI/Fm and the late temperate woodland channel B in West Face Quarry provide, respectively, fluvial and brackish–estuarine limiting maximum RSLAs of <2.5 m OD (G3, Fig. 8(a)) and <2 m OD (A, Fig. 8(a)) dated by AAG to MIS 7 (Penkman et al., 2008a).

Tattershall Castle (WALIS ID RSL 3736, Cohen et al., 2022), representing the IpIIb pollen zone (generally regarded as the Ipswichian climatic optimum; uranium series age of  $120 \pm 6$  ka determined from speleothem in Victoria Cave, northern England (Gascoyne et al., 1981)), is recorded as a salt marsh indicator type providing a SLIP of  $-0.75 \pm 0.71$  m OD (TC, Fig. 8(b)); the sequence at Tattershall Castle has been dated by opercula AAG (Penkman et al., 2011) to MIS 5e, as well as being TL dated to  $114 \pm 16$  ka (Fig. 10(c)). The channel C sequence at Bradley Fen Quarry (Whittlesey; Fig. 1(b), inset) is dated by opercula AAG and records important evidence for the early onset of the Ipswichian climatic optimum in IpIb, for which it provides a fluvial limiting maximum RSLA of <0 m OD (BF3, Fig. 8(b)). Overlying point-bar and overbank deposits provide a fluvial limiting maximum RSLA of 3 m OD for IpIIb. The Deeping St James deposits are an important IpIIb record, with the mammalian fossil assemblage including articulated bones of Palaeoloxodon antiquus (Davies, 1999) and a Dama dama limb bone (unpublished) amongst others that included bear, giant deer and bison. Both these species are part of the Ipswichian Joint Mitnor Cave Mammal Assemblage Zone (Currant and Jacobi, 2011). The Deeping St James deposits are therefore a fluvial equivalent of the Victoria Cave speleothem deposits. These IpIIb deposits provide a fluvial limiting maximum RSLA of <1 m OD (DSJ, Fig. 8(b)), dated by TL to  $117.65 \pm 13.8 \,\text{ka}$  and OSL to  $124.53 \pm 14.9 \,\text{ka}$ (Fig. 9(c)), producing a weighted mean of  $120.81 \pm 14.3$  ka (cf, Victoria Cave date of  $120 \pm 6$  ka). Dating by AAG on B. tentaculata shells using the ratio of alloisoleucine to isoleucine (A/I) method (Keen et al., 1999) and on *B. tentaculata* and *V. piscinalis* shells using the IcPD approach (Penkman, 2005) corroborate a MIS 5e age. At Woolpack Farm in southern Fenland, an IpIIb brackish–estuarine limiting maximum RSLA of <3.5 m OD (WF, Fig. 8(b)) is

dated by OSL to  $121 \pm 22$  ka (Fig. 10(c)). The Woolpack Farm Beds represent a diamicton formed by a flood/tidal surge that includes *Mercuria confusa* as the only brackish molluscan species, but does not contain marine molluscs or C. cf. *fluminalis* (thought to be absent from Britain in Ipswichian

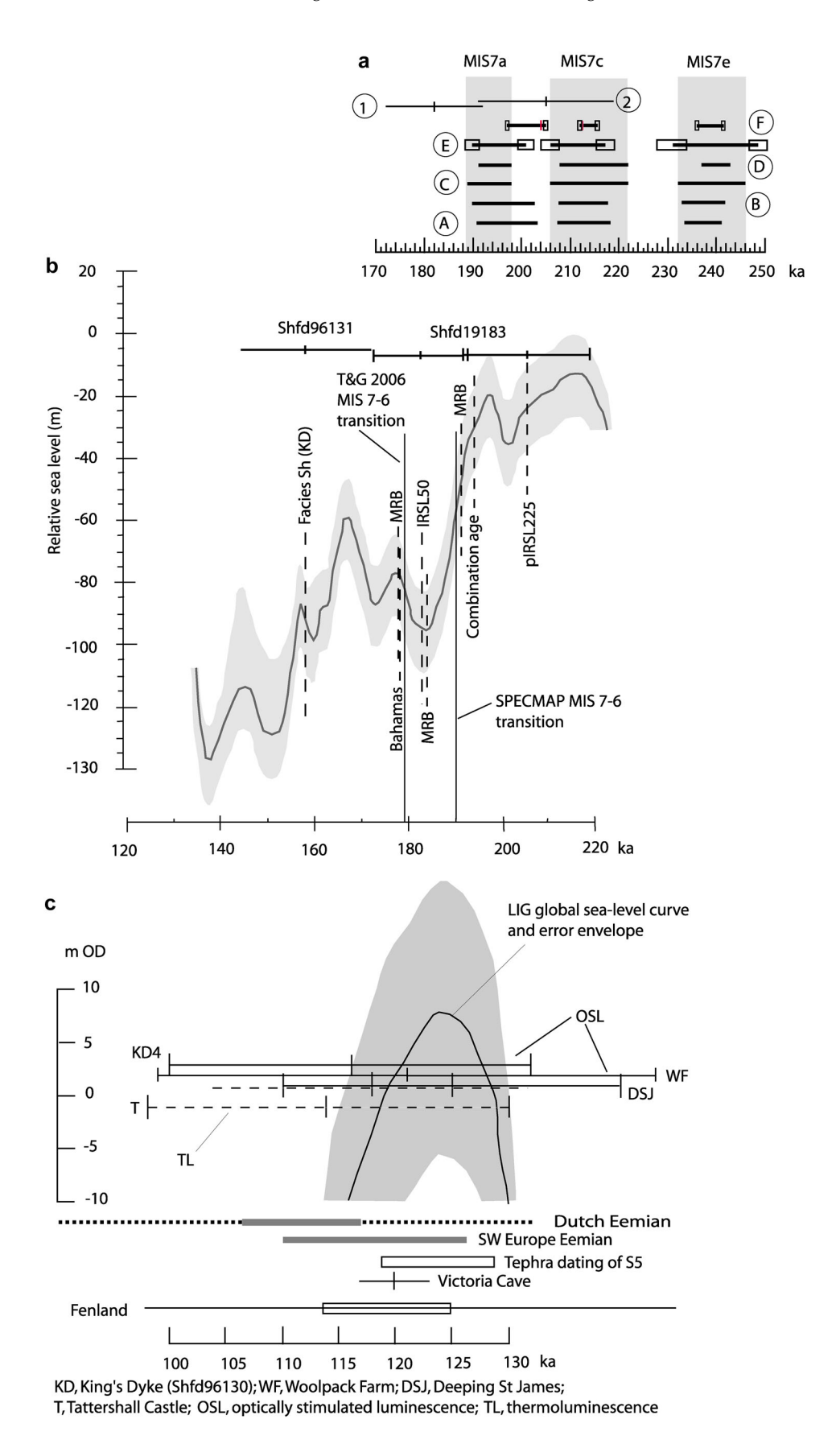


FIGURE 10 Continued.

times; Keen, 1990; Preece, 1995; Meijer and Preece, 2000). At Parkhall Road Quarry, Somersham (Fig. 1(b), inset), where brackish–estuarine sediments are also described as diamictic and contain *M. confusa* but not *C.* cf. *fluminalis*, the underlying beds have produced MIS 5e lower bracketing minimum TL ages (maximum of 130 ka) considered by West et al. (1999) to be too young. These sediments, therefore, provide a possible IpIIb brackish–estuarine limiting maximum RSLA <2 m OD (PR, Fig. 8(b)).

Undated marine-influenced deposits could extend the number of RSLAs in Fenland (Fig. 1; right of the vertical dashed line in Fig. 8): Wretton (Sparks and West, 1970); Block Fen (West et al., 1995a); Knobbs Farm Quarry, Somersham (Fig. 1(b), inset; West et al., 1999); Chatteris and Wimblington (West et al., 1995b). A similar molluscan fauna to that found at Woolpack Farm and Parkhall Road Quarry also occurs in IpIIb brackish-estuarine sediments at Wretton, providing a possible brackish-estuarine limiting minimum RSLA of ≤0.5 m OD (WB, Fig. 8(b)). Similarly, Bed B at Block Fen (West et al., 1995a) is a fully temperate mixed-oak woodland freshwater deposit that lacks C. cf. fluminalis but with M. confusa appearing at the top, providing a possible brackish-estuarine minimum RSLA of -2 m OD (Block Fen B, Fig. 8(b)) and a fluvial limiting maximum RSLA of <-2 m OD. A poorly provenanced AAG A/I ratio of 0.12 on Bithynia shells (Bowen et al., 1989) could also support a MIS 5e age. At a similar height, a C. cf. fluminalis bearing channel fill (Bed D, Fig. 8(a)) with a fully temperate mixed-oak woodland pollen assemblage, that cuts into Bed C, which in turn cuts into Bed A, is interpreted to be younger; however, there does not appear to be any direct evidence that Bed C (and consequently Beds D-F) cuts into Bed B, and, hence, may not be younger.

Older estuarine-brackish deposits at Wretton that represent fully temperate mixed-oak woodland conditions are distinguished from the younger marine-influenced IpII deposits by the presence of C. cf fluminalis. These older deposits contain a similar brackish-marine molluscan fauna to that at section SAO in Fore Fen Quarry and provide a possible brackish-estuarine limiting minimum RSLA of <-1.65 m OD (WA, Fig. 8(a)). Similarly, fully temperate mixed-oak woodland deposits at Knobbs Farm Quarry provide a possible brackish-estuarine limiting minimum RSLA of <-1 m OD (KF, Fig. 8(a)). At Block Fen, the marine-influenced late temperate woodland deposits of Beds E (containing C. cf fluminalis and the common cockle Cerastoderma edule) and F (containing pollen of Chenopodiaceae and Plantago maritima) suggest tidal conditions and provide a possible minimum RSLA of ≤-5.6 m OD (Block Fen, Fig. 8(a)). In addition, the presence of C. cf fluminalis implies a minimum MIS 7 age (Keen, 1990; Preece, 1995; Meijer and Preece, 2000). Similarly, molluscan and foraminifera assemblages in C. cf fluminalis-bearing, late temperate woodland deposits at Wimblington Common (Fig. 8(a)) provide a minimum brackish-marine limiting RSLA of 1 m OD.

#### Stratigraphical grouping of Fenland RSLAs

The following explores the possibility of whether a coherent picture of Fenland penultimate and last interglacial sea-level histories can be arrived at from the evidence available at the RSLA sites (Fig. 8(c)). Although data are sparse and assumptions are required, a fairly coherent picture of upward provision of accommodation space for marine-influenced deposits is apparent for the LIG deposits. Fluvial limiting RSLAs at channel C (BF3, Fig. 8(c)) and Deeping St James (DSJ, Fig. 8(c)) indicate that LIG sea level in Fenland was below modern datum from the early pre-temperate substage (IpIb) to the fully temperate mixed-oak woodland stage (IpIIb). If attribution of Bed B at Block Fen to the LIG is correct, then a minimum Fenland sea level at this time would have been -2 m OD (BIF, Fig. 8(c)), coincident with estuarine-brackish conditions forming from -1.8 to -0.2 m OD at Tattershall Castle (TC, Fig. 8(c)). Marine-influenced IpIIb deposits at Wretton and Parkhall Road Quarry (WB and PR, Fig. 6(c)) share a similar molluscan fauna and stratigraphical position but have not been dated directly, although at the latter, they may be no older than 130 ka. Together, the estuarinebrackish conditions at the above sites form a Fenland RSLA of −2 to +2 m OD for the Ipswichian climatic optimum stage, commensurate with the maximum 3.5 m brackish-estuarine limiting RSLA of the Woolpack Farm Beds (W, Fig. 8(c)) flood deposits, and as confirmed by the SLIP of  $-0.75 \pm 0.71$  m OD at Tattershall Castle. At present, there are no viable records of marine-influenced deposits attributable to IpIII, although a possible undated fluvial limiting RSLA of ≤4.75 m OD may have been recorded at Chatteris New Road (Ch, Fig. 6(c); West et al., 1995b). The OSL date of 116 ka at Whittlesey (KD4, Fig. 8(c)) also could represent the late-temperate stage, suggesting that peak RSL then would have been no more than 3.75 m OD.

Luminescence dates and the pollen record at both Northam Pit and Morston raised beach appear to provide a record of upward provision of accommodation space at the culmination of MIS 7 (Fig. 8(c)). A peak RSL of  $2.5 \pm 1$  m OD is recorded at Morston raised beach (Fig. 8(a)), commensurate with a minimum RSLA of 2.5 m at Northam Pit, where marine proximal conditions were recorded at 1.9 m OD. The above-ordnance-datum records at Northam Pit and Morston raised beach, however, appear to contradict global reconstructions of MIS 7 climatic substage sealevel peaks (Figs. 9(b) and 10; discussed in detail below). Furthermore, it is difficult to reconcile the Fenland penultimate interglacial RSLAs recorded at West Face Quarry and those for the River Great Ouse catchment with a single penultimate interglacial transgression without invoking specific complex combinations of responses to regional glacio-isostatic adjustment (GIA) as well as global climate and sea level. Therefore, it is more likely that the less coherent picture of penultimate interglacial sea level provided by Fenland RSLAs results from the complexity of the MIS 7 climatic stage (Fig. 9). Consequently, it is worthwhile to

**Figure 10.** (a) The (1) IRSL<sub>50</sub> and (2) pIRSL<sub>225</sub> dates from Northam Pit plotted against reported MIS 7 substage time spans: (greyshade) Candy and Schreve (2007), adopted from (C) Martinson et al. (1987); (A) Monaco et al. (2022); (B) Head and Gibbard (2015); (D) Rodrigues et al. (2017); (E) Dutton et al. (2009); (F) Wendt et al. (2021). Uncertainties reported by Wendt et al. (2021) and Monaco et al. (2022) are shown as boxes at either end of the time spans. (b) The IRSL<sub>50</sub> and pIRSL<sub>225</sub> dates from Northam Pit and OSL date from section KD2 at King's Dyke Quarry plotted against the global RSL curve of Waelbroeck et al. (2002). Also plotted are reported anomalies/uncertainties concerning the MIS 7–6 transition. 'Bahamas' denotes the warm temperature anomaly reported by Robinson et al. (2002); T&G 2006 the radiometrically calibrated U–Th age of Thompson and Goldstein (after Hoare et al., 2009); MRB, the median OSL ages calculated for the Morston Raised Beach. (c) Fenland Ipswichian luminescence dates plotted against the MIS 5e sea-level peak of Waelbroeck et al. (2002). Solid lines indicate OSL determinations and dashed lines those determined by thermoluminescence (TL). Also shown are plots of the distribution of Dutch Eemian (Peeters et al., 2016) and Fenland Ipswichian median luminescence dates, tephra dating of Sapropel S5 (126.4 ± 2.9 ka to 121.8 ± 2.9 ka) in the eastern Mediterranean (Satow et al., 2020), on which global deep-sea and southwest Europe Eemian timescales are based, and the U-series date from Victoria Cave, northern England (Gascoyne et al., 1981). KD, King's Dyke (Shfd96130); DSJ, Deeping St James (Keen et al., 1999); T, Tattershall Castle (Holyoak and Preece, 1985); WF, Woolpack Farm (Gao et al., 2000).

consider in detail the constraints on MIS 7 sea-level reconstructions provided by the Fenland RSLAs.

At West Face Quarry, facies St–FL/Fm (at WF4) and facies Gcm/Fm, Sm and Gt–St (at WF3) respectively overlie and cut into channel B deposits, so both are undoubtedly younger. At log F1 (Fig. 8(a)) clast-lithology evidence testifies to post-depositional weathering of channel B deposits, which resulted in Fe-cementation, absence, or near absence of ironstone clasts, notable increase in flint and reduction of limestone, including weathered limestone clasts (Langford et al., 2004b). Reworked Fe-cemented (including shell-bearing) aggregates at the base demonstrate that the post-depositional weathering pre-dated deposition of facies Gcm/Fm, suggesting a significant hiatus between it and channel B. Thus, at least two separate MIS 7 climatic substages appear to be represented in the marine-influenced deposits at West Face Quarry.

As depicted in Fig. 8(a), (c) there are two obvious anomalies: (i) below ordnance datum brackish-estuarine limiting RSLAs are restricted to the River Great Ouse catchment (but note that the March Gravel occurs to a depth of -3.1 m OD at Eye Green (Booth, 1982) and that below 1.7 m OD at Northam Pit was obscured); (ii) marine-influenced deposits of the late temperate woodland stage lie above as well as below marineinfluenced deposits of the fully temperate mixed-oak woodland stage. Both could be explained simply as an artefact of the sparse data set or the vagaries of accommodation and preservation potential as a result of climate-driven fluvial response and GIA. A possible explanation for the former, however, is that high-energy discharge and high sediment yield associated with MIS 8 drainage reorganisation infilled low-lying accommodation space in the River Nene and Welland catchments (Langford, 1999, 2004, 2012, 2018). In contrast, the River Great Ouse would have been largely unaffected by this, and as drainage through The Wash persisted, so would the potential for downcutting and provision of low-lying accommodation space associated with falling sea level. Whatever the explanation for this provision of low-lying accommodation space, the sequence of infilling is difficult to establish with the data available.

Although the AAG dating of Bed 3c fauna at Somersham provides an upper bracketing age for underlying Bed 2(m), establishing an age equivalent to MIS 7 is not straightforward. Its assignment to MIS 7, thus far, is based on the presence of C. cf. fluminalis. However, it can be argued that despite numerous pollen analyses and reliance on pollen assemblages for stratigraphical interpretation at this and related Fenland sites (Sparks and West, 1970; West et al., 1994; West et al., 1995a, 1995b, 1999), the absence so far of Hoxnian pollen indicator species implies a MIS 7 age for Bed 2(m), as well as for all associated C. cf. fluminalis-bearing deposits. Although unravelling the sequence of Fenland MIS 7 deposits is unlikely, there are some stratigraphical indications. Interpreted tidal conditions suggest marine proximity and thus the late temperate marine-influenced deposits providing a possible minimum RSLA of  $\leq -5.6$  m OD at Block Fen (BIF, Fig. 8(c)) are unlikely to correspond to the late temperate estuarine minimum 2.5 m OD RSLA at Northam Pit, with the possibility that the former represents an earlier MIS 7 substage (7c or 7e). A further consideration arises from the difference between the microfauna assemblages of beds 2(m) and 3(c) in Fore Fen Quarry (West et al., 1994; West et al., 1999). This could be attributable to a different downstream facies being eroded and deposited upstream, which would account for the greater variety of habitats represented by the microfauna of Bed 3c and its evidence of southerly flow (G.F. Dardis, personal communication, 1991). Alternatively, it could be attributed solely to a southerly flowing stream reworking overlying

sediments deposited during a transgression later than Bed 2(m), or to a mixture of later transgressive deposits and earlier different downstream facies.

### Implications for the marine-influenced March Gravel

As the sedimentary sequences at Northam Pit and sections KD2 and KD4 at Whittlesey are mapped as March Gravel and that represented by Bed 3c at Somersham (Figs. 1 and 2) is considered an equivalent, especially in terms of depositional process (West et al., 1994), the results of this study have implications for the marine status of the March Gravel (Maddy, 1999; Rose, 2015). Both the Northam Pit and Bed 3c sequences contain C. cf. fluminalis, whereas those at KD2 and KD4 do not. The reworked marine-brackish fauna component of the sequence at Northam Pit (RWm, Fig. 8(a)) has a maximum age of MIS 7c and a minimum age of MIS 2. At KD2, the relevant part of the sequence (facies PGcs to Fd) has a maximum age of MIS 7 and a minimum of MIS 6; at KD4, it has an age equivalent to MIS 5e. Taking all these factors into consideration, sediments mapped as March Gravel likely represent a patchwork of different-aged, marine-influenced deposits assembled by a variety of processes, as argued by West et al. (1994, 1999).

#### Comparison with global records

It is difficult to ascertain the global highstand event represented at each Fenland site because of the combination of the significant uncertainties associated with both the age-estimate and the error margins for modelled sea-level data (Figs. 9(b) and 10). The MIS 7 luminescence ages at Northam Pit embrace a sea level range of about 60 m (Spratt and Lisiecki (2016) calculate a similar range), and for MIS 5e at Whittlesey, a range of about 80 m (Fig. 8(b); Kopp et al. (2009) and Spratt and Lisiecki (2016) calculate a range of no more than 50 m). In addition, as most of the data concerned are RSLAs, it is not possible to establish a reliable RSL indicator. Therefore, the discussion below does not engage with the additional uncertainties of coastal configuration, GIA and geological terrane processes (i.e., crustal deformation), all of which would be highly speculative in this instance. None of the dated deposits considered here is more than ca. 3-5 m above or below the present local ordnance datum. Global sea level curves (including errors) reconstruct penultimate interglacial global sea levels between ca. -30 m and +15 m and LIG sea levels between ca. -10 and +20 m (Bintanja et al., 2005; Bates et al., 2014; Grant et al., 2014; Spratt and Lisiecki, 2016). Thus, the error margins are already significant, and adding further speculative adjustments to the Fenland data is not appropriate.

#### Marine isotope stage 7

The estuarine deposits at Northam Pit represent a minimum RSLA of 2.5 m OD (Fig. 8(a)). This appears to be several metres above MIS 7 global sea-level highstands, commonly regarded as being lower than modern datum (Imbrie et al., 1984; Waelbroeck et al., 2002; Siddall et al., 2003; Bintanja et al., 2005; Rohling et al., 2009). It should be noted, however, that all post-Anglian/Elsterian (MIS 12) marine transgressions reached onshore areas of the Netherlands, with the exception of MIS 9 (Meijer and Cleveringa, 2009), and Proctor and Smart (1991), suggest a MIS 7 age for 7.2 m OD sea level recorded at Corbridge Cave (Torbay, Devon). This could relate to either local ground movement or to errors in the global reconstructions.

17/11/2025, See the Terms and Conditions (https://oinleibbary.wiley.com/doi/01.0102/js;70025 by NCE, National Institute for Health and Care Excellence, Wiley Online Library or [17/11/2025]. See the Terms and Conditions (https://onlineibbary.wiley.com/terms-and-conditions) on Wiley Online Library for rules of use; OA articles are governed by the applicable Creative Commons License

For example, Briant et al. (2024) attribute the similarity in elevation of the MIS 7 Brighton-Norton Formation shore platform (absolute elevation ca. 7.2 m OD, RSL corrected for indicative meaning ca. 5.7 m OD) to the MIS 5e shore platform at Bembridge, Isle of Wight, UK (absolute elevation ca. 6 m OD, RSL corrected for indicative meaning ca. 5.3 m OD) to glacioisostatic adjustment during MIS 6. Alternatively, in relation to global reconstructions, there are various exceptions to the common perception of low MIS 7 sea-level highstands (Gallup et al., 1994, 2002; Edwards et al., 1997; Lea et al., 2002; Thompson and Goldstein, 2005; Spratt and Lisiecki, 2016), and Dutton et al. (2009) have demonstrated that differences occur not only in the magnitude but also the timing of the MIS 7 highstands, particularly for MIS 7c, depending on the proxy sealevel measure used (Fig. 10(a)). In addition, Hoare et al. (2009) noted the discrepancy between the 189.6 ka age for the MIS 7a-6 transition in the SPECMAP timescale (Fig. 10(b); which is close to most of those depicted in Fig. 10(a)) and the 179.2 ka radiometric age calculated by Thompson and Goldstein (2005). Under these circumstances, and given the rarity of regional MIS 7 sea-level indicators, the reliably dated RSLA at Northam Pit should be regarded as a genuine approximation and not an anomaly, although it should be remembered that local indicators only record RSL, not global sea level.

Of the three median IRSL ages reported for the estuarine sequence at Northam Pit, the match between the median combination age of 194 ka and the 200 ka global sea-level highstand is closest (Figs. 9(b) and 10(b)). This still presents a problem because, rather than plotting above present, it plots up to 20 m below, on the falling limb of the MIS 7-6 transition. As noted above, the global picture may not reflect the immediate regional situation. For example, the median age range of 180-191 ka for the Morston raised beach (Fig. 10b, MRB) could suggest that high RSL, up to 5 m OD, persisted in the North Sea into the MIS 7-6 transition (Hoare et al., 2009). A suggestion that could be supported by marine-influenced deposits found on both sides of the English Channel with evidence for cooling prior to or during RSL fall at the MIS 7-6 transition (Lefebvre, 1993; Bates et al., 2000; Jones and Whittaker, 2010). Furthermore, a complex ending to MIS 7 was reported by Robinson et al. (2002), who recorded interglacial conditions at 178.4 ka in the Bahamas, some 10 ka younger than ages of ca. 190 ka determined from orbitally tuned and coral/speleothem data (Fig. 10(b)).

#### Marine isotope stage 5e

The maximum brackish-estuarine limiting RSLA of 3.75 m at KD4 suggests a lower LIG peak RSL than the global MIS 5e highstand of between 6 and 8 m above modern datum determined by Waelbroeck et al. (2002; Fig. 9(b)). A determination that corresponds closely with the >6.6 m but <9.4 m of Kopp et al. (2009) and up to 9 m of Giaccio et al. (2023), but is slightly more than the 3-6 m above modern datum of Siddall et al. (2010) considered to have been attained by 126 ka. The 3.75 m maximum at KD4 falls within the range of Siddall et al. (2010), albeit 10 ka later, and is similar to the 5.8 m recorded at Corbridge Cave (Proctor and Smart, 1991), the few metres above modern datum recorded for Majorca and the western Mediterranean (Ginés et al., 2001; Bardají et al., 2009; see fig. 3 of Antonioli, 2012), as well as that recently modelled for the Bahamas by Dyer et al. (2021) of no more than 5.3 m and determined from Bahamian fossil coral reefs by Dumitru et al. (2023) for 117 ka of about -1 to about 4 m.

When the MIS 5e OSL age of 116 ka from KD4 is plotted against the global sea-level curve, a significant lag is apparent (Fig. 10(c)). This is not necessarily an artefact of the statistical

uncertainties associated with the OSL date, but could be further evidence of a complex picture of climatic and sea-level lags characterising the LIG, as discussed by Langford et al. (2017). For example, a 5000-year lag between commencement of the Southwest Europe Eemian (based on appearance of the Blake Event in the benthic record off the Iberian coast) and that in global deep-sea records (based on the onset of sapropel S5 in the eastern Mediterranean) and a further 5000 year lag between commencement of the Dutch Eemian (based on the appearance of the Blake Event in the fluvial record at Rutten in the type site area) and the Southwest Europe Eemian (Shackleton, 1969; Sánchez-Goñi et al., 1999; Shackleton et al., 2002, 2003; Lisiecki and Raymo 2005; Sier et al., 2015). The range of median luminescence ages for Fenland as a whole appears to lag global peak sea level and the formation of sapropel S5, but is compatible with the age range of the Southwest Europe Eemian, whereas peak Fenland sea level seems coincident with the onset of the Dutch Eemian.

#### Proposed implications for Fenland evolution

The results of this study build upon recent investigations into late Middle to Upper Pleistocene deposits of the Peterborough area and can provide further intuitive insights into the evolution of Fenland and hence sediment delivery to the southern North Sea basin. It is envisaged here that Fenland MIS 7 evolution proceeded on a landscape sculpted by glacially influenced drainage reorganisation in MIS 8 (for alternative reconstructions see Gibbard et al. (2018) and White et al. (2017)). As a result, valleys of the Welland and Nene were infilled with concomitant sand and gravel spreads on interfluves and the western edge of Fenland, with large fluxes of sediment being delivered through The Wash to the southern North Sea basin.

In the early part of MIS 7, accommodation potential for marine-influenced sediments was provided primarily below ordnance datum in the lower River Great Ouse and its tributaries on the eastern side of Fenland, and probably of Fenland rivers in the vicinity of The Wash. The tidal limit lay downstream of Whittlesey during the late temperate woodland phase of this early transgression. Regression and a lengthy period of subaerial weathering, followed by a cold phase when global sea level fell by about 80 m and the Polar Front migrated south of 50° N (Fabian et al., 2023). Subsequent accommodation potential for marine-influenced sediments was provided by RSL rising to at least 2.5 m above OD. The presence of A. perlucida at Northam Pit suggests either an intermittent (Hijma et al., 2012) or viable (Meijer and Cleveringa, 2009) link between the North Sea and English Channel at this time. The latest influx of brackish-marine microfauna at Whittlesey, also containing A. perlucida, indicates that the tidal limit lay downstream late in MIS 7, with sea level similar to present.

Early in MIS 6, channel incision into bedrock and infilling are evident at Whittlesey (Langford et al., 2014b). At 158 ka, just prior to when the Polar Front had migrated south of 50° N (Fabian et al., 2023), coincident with major ice rafting from the British-Irish Ice Sheet (BIIS), drainage at Whittlesey was directed eastward through The Wash, and continued through The Wash until after 148 ka (Gibbard et al., 2021). The Polar Front was also situated south of 50° N at the termination of both MIS 6 and 2, coincident with terminal ice rafting of the BIIS. Impingement of ice on the north Norfolk coast in MIS 6 did not occur until 141 ka (i.e., the European Warthe glacial advance), some time later than what appears to be the maximum ice extent at about 155 ka (i.e., end of the European Drenthe glacial advance). This situation is somewhat similar to events of the last glaciation in the North Sea, when ice impingement of the north Norfolk coast and impoundment of drainage through The Wash occurred during a later readvance phase rather than at ice-maximum conditions (Roberts et al., 2018). Fenland experienced a profound change in the provision of accommodation space when impoundment at The Wash led to drainage reorganisation, with flow to the south recorded at Whittlesey and Somersham. Extensive braidplains formed as cut-and-fill channels migrated laterally, reworking existing gravel and sand sheets as well as incorporating contemporary material. Hence, as evident at Somersham, the March Gravel could mostly represent local reworking of MIS 7 marine-influenced deposits in MIS 6.

Unlike early MIS 7, low-lying accommodation space in Fenland was not available in the subsequent MIS 5e interglacial, as drainage became re-established through The Wash by singlethread sinuous streams migrating laterally across remnant braidplain deposits. Most accommodation space early in the interglacial would have been provided within channels in the vicinity of The Wash and seaward; thus, with ongoing transgression, preservation potential was extremely low. There is local evidence of marine ingress in the fully temperate mixed-oak woodland phase (Tattershall Castle and possibly Block Fen, Fig. 8), otherwise, MIS 5e marine-influenced deposits in Fenland so far recorded are flood or tidal surge deposits some distance upstream of the tidal limit. Apart from the maximum RSLA of 3.75 m OD at Whittlesey, there is as yet no evidence of the high sea levels generally attributed to the LIG. In Fenland the Ipswichian optimum was coincident with the Southwest Europe and global LIG optimum at a time when sea level was lower than modern datum, but peak Fenland RSL seems coincident with the later onset of the Northwest Europe LIG.

#### **Conclusions**

Current modelled palaeo-sea-level curves for MIS 7 and 5e have large uncertainties. One reason for this is inadequate direct age control stemming from the scarcity of interglacial sites with critical data on the actual sea level at the time of deposition. This study has successfully distinguished between Fenland MIS 7 and 5e sites with records of marine-influenced deposits: five reliably dated RSLA data points, plus four that are not dated, and one SLIP for each interglacial stage. These data should provide useful regional input to, and hence improve the relevance of, global reconstructions of late Middle and Late Pleistocene sea level. Fenland results and global records diverge in terms of MIS 7 peak sea level and the timing of the MIS 5e peak sea level, but these divergences must be weighed against the uncertainties in the modelled palaeo-sealevel and age-estimate results.

A key finding from this research is that the RSLAs assigned to both MIS 7 and 5e sites in Fenland are largely found within the same elevation range of ca. -3 to +4 m OD. This similarity in elevation has also been seen to the north at Kirmington (Fig. 3), where combined marine-/terrestrial-limited RSLAs of just below present to 5 m OD have upper and lower bracketing ages of MIS 8 and MIS 2. Straw (2018) favoured MIS 7 RSL to be slightly below present and MIS 5e RSL to be slightly above. To the south, the Sussex coast (including the Hampshire Basin; Briant et al., 2024), the Channel Islands (Keen et al., 1996) and northwest France (Laforge, 2012) also record similar elevations for MIS 7 and 5e RSL. It is possible that global sea levels for MIS 7 may have been underestimated, as discussed above, but for the Sussex coast, Briant et al. (2024) assign this similarity to GIA during MIS 6. These findings, however, do not necessarily apply elsewhere because of the different geological terranes involved (Fig. 3). Although the exact configurations of the MIS 8 and 6 ice sheets in the vicinity of Fenland are uncertain, localised glacial

overriding in eastern Fenland in MIS 6 could have affected glacial loading of the LBP and forebulge warping, resulting in a different GIA than that in MIS 8. Another potential source of differential GIA is the transfer of sediment load of Fenland rivers from the EMF to the Brabant Massif segment of the LBP as a consequence of the impoundment of The Wash in MIS 6. The apparent coherent picture of upward provision and infilling of accommodation space evident from MIS 5e deposits in Fenland, however, could argue against spatial differentiation of GIA attributable to the MIS 6 glaciation. As the MIS 8 glacial footprint appears to be less extensive locally, the case for spatial differentiation of GIA in Fenland is less likely than for MIS 6. Consequently, the lack of a coherent picture of upward creation and filling of accommodation space for Fenland MIS 7 deposits probably reflects the complexity of that interglacial.

Acknowledgements. A QRA Quaternary Research Fund grant funded the IRSL dating at Northam Pit. Sam Presslee carried out the IcPD analysis of *Bithynia tentaculata* opercula from King's Dyke, West Face and Fore Fen quarries as part of a project that has received funding from the European Research Council (ERC) under the European Union's Horizon 2020 research and innovation programme (grant agreement No. 865222—EQuaTe). David Penney (formerly at Aarhus University) analysed the ostracods from section KD2. We are grateful for the helpful comments made by the three reviewers.

#### Data availability statement

Data in this study have been included in the Supplementary Material and will be available on the NOAA data repository upon publication: https://www.ncei.noaa.gov/pub/data/paleo/aar/.

For the purpose of open access, the author has applied a Creative Commons Attribution (CC BY) licence to any Author Accepted Manuscript version arising from this submission.

#### **Supporting information**

Additional supporting information can be found in the online version of this article.

Supplementary Tables S1–S5.

#### References

Aldridge, D.C. (1999) The morphology, growth and reproduction of Unionidae (Bivalvia) in a Fenland waterway. *Journal of Molluscan Studies*, 65, 47–60.

Anderton, R., Bridges, P.H., Leeder, M.R. & Sellwood, B.W. (1979) *A dynamic stratigraphy of the British Isles: a study in crustal evolution*. London: George Allen & Unwin. p. 301

Antonioli, F. (2012) Sea level change in western-central Mediterranean since 300 kyr: comparing global sea level curves with observed data. *Alpine and Mediterranean Quaternary*, 25(1), 15–23.

Athersuch, J., Horne, D.J. & Whittaker, J.E. (1989) Marine and brackish water ostracods. In: *Synopses of the British fauna (New Series)*, vol. 43, 8 pls. Leiden: E.J. Brill, 343 pp.

Baden-Powell, D.F.W. (1934) On the marine gravels at March, Cambridgeshire. *Geological Magazine*, 71(v), 193–219.

Bardají, T., Goy, J.L., Zazo, C., Hillaire-Marcel, C., Dabrio, C.J., Cabero, A. et al. (2009) Sea level and climate changes during OIS 5e in the western Mediterranean. *Geomorphology*, 104, 22–37.

Bateman, M.D. & Catt, J.A. (1996) An absolute chronology for the raised beach and associated deposits at Sewerby, East Yorkshire, England. *Journal of Quaternary Science*, 11, 389–395.

Bateman, M., Briant, R.M., Langford, H. et al. (2020) Determining the age of the late Middle Pleistocene marine March Gravel of eastern England. *Quaternary Newsletter*, 151, 13–20.

Bateman, M.D., Boulter, C.H., Carr, A.S., Frederick, C.D., Peter, D. & Wilder, M. (2007) Detecting post-depositional sediment disturbance in sandy deposits using optical luminescence. *Quaternary Geochronology*, 2, 57–64.

10991417, Downloaded from https://onlinelibrary.wiley.com/doi/10.1002/gs.70025 by NCE, National Institute for Health and Care Excellence, Wiley Online Library on [17/1/2025], See the Terms and Conditions (https://onlinelibrary.wiley.com/erms-and-conditions) on Wiley Online Library for rules of use; OA articles are governed by the applicable Creative Commons.

- Bates, M.R., Bates, C.R., Gibbard, P.L., Macphail, R.I., Owen, F.J., Parfitt, S.A. et al. (2000) Late Middle Pleistocene deposits at Norton Farm on the West Sussex coastal plain, southern England. *Journal of Quaternary Science*, 15, 61–89.
- Bates, S.L., Siddall, M. & Waelbroeck, C. (2014) Hydrographic variations in deep ocean temperature over the mid-Pleistocene transition. *Quaternary Science Reviews*, 88, 147–158.
- BGS. (1980) British Geological Survey (England and Wales): Ely Sheet 173, Solid and Drift Edition, 1:50,000 Series. Keyworth: British Geological Survey.
- BGS. (1984) British Geological Survey (England and Wales): Peterborough sheet 158, solid and drift edition, 1:50,000 Series. Keyworth: British Geological Survey.
- BGS. (1995a) British Geological Survey (England and Wales): Wisbech sheet 159, solid and drift edition, 1:50,000 series, Keyworth: British Geological Survey.
- BGS. (1995b) British Geological Survey (England and Wales): Ramsey sheet 172, solid and drift edition, 1:50,000 provisional series. Keyworth: British Geological Survey.
- Bintanja, R., van de Wal, R.S.W. & Oerlemans, J. (2005) Modelled atmospheric temperatures and global sea levels over the past million years. *Nature*, 437, 125–128.
- Boomer, I., Horne, D.J. & Slipper, I.J. (2003) The use of ostracods in palaeoenvironmental studies, or what can you do with an ostracod shell? In: Park, L.E. & Smith, A.J. (Eds.) *Bridging the gap: trends in the ostracode biological and geological sciences, The Paleontological Society papers*, vol. 9. Cambridge: Cambridge University Press, pp. 153–179.
- Booth, S.J. (1982) The sand and gravel resources of the country around Whittlesey, Cambridgeshire. Description of 1:25,000 sheets TF 20 and TL 29. Institute of Geological Sciences. Mineral Assessment Report 93. 109 pp.
- Boreham, S., White, T.S., Bridgland, D.R., Howard, A.J. & White, M.J. (2010) The Quaternary history of The Wash fluvial network, UK. *Proceedings of the Geologists' Association*, 121(4), 393–409.
- Bowen, D.Q., Hughes, S., Sykes, G.A. & Miller, G.H. (1989) Land–sea correlations in the Pleistocene based on isoleucine epimerization in non-marine molluscs. *Nature*, 340, 49–51.
- Briant, R.M., Bates, M.R., Robertson, J., Schwenninger, J.L. & Whittaker, J.E. (2024) Indicative meanings of geological sea-level indicators in the Solent region and Sussex coast (south coast of England) and implications for uplift rates. *Journal of the Geological Society*, 181, jgs2023-120. Available from: https://doi.org/10.1144/jgs2023-120
- Bridgland, D.R., Davey, N.D.W. & Keen, D.H. (1991) Northam Pit, Eye, near Peterborough. In: Lewis, S.G., Whiteman, C.A. & Bridgland, D.R. (Eds.) Central East Anglia and the Fen Basin, Field Guide. London: Quaternary Research Association, pp. 173–183.
- Busschers, F.S., Kasse, C., van Balen, R.T., Vandenberghe, J., Cohen, K.M., Weerts, H.J.T. et al. (2007) Late Pleistocene evolution of the Rhine-Meuse system in the southern North Sea basin: imprints of climate change, sea-level oscillation and glacio-isostacy. *Quaternary Science Reviews*, 26(25–28), 3216–3248.
- Buylaert, J.-P., Jain, M., Murray, A.S., Thomsen, K.J., Thiel, C. & Sohbati, R. (2012) A robust feldspar luminescence dating method for Middle and Late Pleistocene sediments. *Boreas*, 41, 435–451.
- Candy, I. & Schreve, D. (2007) Land–sea correlation of Middle Pleistocene temperate sub-stages using high-precision uraniumseries dating of tufa deposits from southern England. *Quaternary Science Reviews*, 26, 1223–1235.
- Castleden, R. (1980) The second and third terraces of the River Nene. *Mercian Geologist*, 8(1), 29–46.
- Cohen, K.M., Cartelle, V., Barnett, R., Busschers, F.S. & Barlow, N.L.M. (2022) Last Interglacial sea-level data points from Northwest Europe. *Earth System Science Data*, 14, 2895–2937.
- Cohen, K.M., Gibbard, P.L. & Weerts, H.J.T. (2014) North Sea palaeogeographical reconstructions for the last 1 Ma. *Netherlands Journal of Geosciences*, 93, 7–29.
- Crisp, M.K. (2013) Amino acid racemization dating: method development using African ostrich (*Struthio camelus*) eggshell. PhD Thesis, University of York.
- Currant, A.P. & Jacobi, R. (2011) The mammal faunas of the British Late Pleistocene. In: Ashton, N., Lewis, S.G. & Stringer, C. (Eds.) *Developments in Quaternary Sciences*, vol. 14. Amsterdam: Elsevier, pp. 165–180.

- Darling, K.F., Schweizer, M., Knudsen, K.L., Evans, K.M., Bird, C., Roberts, A. et al. (2016) The genetic diversity, phylogeography and morphology of Elphidiidae (Foraminifera) in the northeast Atlantic. *Marine Micropaleontology*, 129, 1–23.
- Davies, P. (1999) The Deeping St James elephant (*Palaeoloxodon antiquus*) and other mammalian fossils. In: Langford, H.E. (Compiler). *Cool Peterborough: Peterborough in the ice ages.* Peterborough: Langford Editorial Services, pp. 23–27.
- Douglas, T.D. (Ed.) (1981) Field guide to the East Midlands region. Leicester: Quaternary Research Association.
- Dumitru, O.A., Dyer, B., Austermann, J., Sandstrom, M.R., Goldstein, S.L., D'Andrea, W.J. et al. (2023) Last interglacial global mean sea level from high-precision U-series ages of Bahamian fossil coral reefs. *Quaternary Science Reviews*, 318, 108287.
- Dutton, A., Bard, E., Antonioli, F., Esat, T.M., Lambeck, K. & McCulloch, M.T. (2009) Phasing and amplitude of sea-level and climate change during the penultimate interglacial. *Nature Geoscience*, 2(5), 355–359.
- Dutton, A., Carlson, A.E., Long, A.J., Milne, G.A., Clark, P.U., DeConto, R. et al. (2015) Sea-level rise due to polar ice-sheet mass loss during past warm periods. *Science*, 349, 153.
- Dyer, B., Austermann, J., D'Andrea, W.J., Creel, R.C., Sandstrom, M.R., Cashman, M. et al. (2021) Sea-level trends across The Bahamas constrain peak last interglacial ice melt. *Proceedings of the National Academy of Sciences*, 118(33), e2026839118.
- Edwards, R.L., Cheng, H., Murrell, M.T. & Goldstein, S.J. (1997) Protactinium-231 dating of carbonates by thermal ionization mass spectrometry: implications for Quaternary climate change. *Science*, 276, 782–786.
- Fabian, S.G., Gallagher, S.J. & DeVleeschouwer, D. (2023) British—Irish Ice Sheet and polar front history of the Goban Spur, offshore southwest Ireland over the last 250 000 years. *Boreas*, 52, 476–497.
- Galbraith, R.F. & Green, P.F. (1990) Estimating the component ages in a finite mixture. *Nuclear Tracks and Radiation Measurements*, 17, 197–206.
- Galbraith, R.F., Roberts, R.G., Laslett, G.M., Yoshida, H. & Olley, J.M. (1999) Optical dating of single and multiple grains of quartz from Jinmium rock shelter, northern Australia, Part I: experimental design and statistical models. *Archaeometry*, 41, 339–364.
- Gallois, R.W. (1988) Geology of the country around Ely. Memoir of the British Geological Survey, Sheet 173, England and Wales. London: HMSO.
- Gallois, R.W. (1994) Geology of the country around King's Lynn and the Wash: Memoir of the British Geological Survey, Sheet 145 and part of 129, England and Wales. London: HMSO.
- Gallup, C.D., Cheng, H., Taylor, F.W. & Edwards, R.L. (2002) Direct determination of the timing of sea level change during Termination II. *Science*, 295, 310–313.
- Gallup, C.D., Edwards, R.L. & Johnson, R.G. (1994) The timing of high sea levels over the past 200,000 years. *Science*, 263, 796–800.
- Gao, C., Keen, D.H., Boreham, S., Coope, G.R., Pettit, M.E., Stuart, A.J. et al. (2000) Last Interglacial and Devensian deposits of the River Great Ouse at Woolpack Farm, Fenstanton, Cambridgeshire, UK. *Quaternary Science Reviews*, 19, 787–810.
- Gascoyne, M., Currant, A.P. & Lord, T.C. (1981) Ipswichian fauna of Victoria Cave and the marine palaeoclimatic record. *Nature*, 294, 652–654.
- Giaccio, B., Bini, M., Isola, I., Hu, H.M., Rolfo, M.F. Chuan-Chou, S. et al. (2023) Constraining the end of the Last Interglacial (MIS 5e) relative sea-level highstand in central Mediterranean: new data from Grotta delle Capre, central Italy. *Global and Planetary Change*, 232, 104321.
- Gibbard, P.L., Bateman, M.D., Leathard, J. & West, R.G. (2021) Luminescence dating of a late Middle Pleistocene glacial advance in eastern England. *Netherlands Journal of Geosciences*, 100, e18.
- Gibbard, P.L., West, R.G. & Hughes, P.D. (2018) Pleistocene glaciation of Fenland, England, and its implications for evolution of the region. *Royal Society Open Science*, 5, 170736.
- Ginés, J., Fornós, J.J., Ginés, A., Gracia Alonso, F., Delitala, C., Taddeucci, A. et al. (2001) Els espeleotemes freàtics de les coves litorals de Mallorca: canvis del nivell de la Mediterránia i paleoclima en el Pleistocé superior. In: Pons, G.X. & Guijarro, J.A. (Eds.) *El canvi climàtic: passat, present i futur*, vol. 9. Spain: Societat d'Història Natural de les Balears, pp. 33–52.

- Glennie, K.W. (1990) Introduction to the petroleum geology of the North Sea. Oxford: Blackwell Scientific Publications.
- Grant, K.M., Rohling, E.J., Ramsey, C.B., Cheng, H., Edwards, R.L., Florindo, F. et al. (2014) Sea-level variability over five glacial cycles. *Nature Communications*, 5, 5076.
- Guérin, G., Mercier, N. & Adamiec, G. (2011) Dose-rate conversion factors: update. *Ancient TL*, 29, 5–8.
- Head, M.J. & Gibbard, P.L. (2015) Early–Middle Pleistocene transitions: linking terrestrial and marine realms. *Quaternary International*, 389, 7–46.
- Hijma, M.P., Cohen, K.M., Roebroeks, W., Westerhoff, W.E. & Busschers, F.S. (2012) Pleistocene Rhine–Thames landscapes: geological background for hominin occupation of the southern North Sea region. *Journal of Quaternary Science*, 27, 17–39.
- Hill, R.L. (1965) Hydrolysis of proteins. Advances in Protein Chemistry, 20, 37–107.
- Hoare, P.G., Gale, S.J., Robinson, R.A.J., Connell, E.R. & Larkin, N.R. (2009) Marine Isotope Stage 7–6 transition age for beach sediments at Morston, north Norfolk, UK: implications for Pleistocene chronology, stratigraphy and tectonics. *Journal of Quaternary Science*, 24, 311–316.
- Holyoak, D.T. & Preece, R.C. (1985) Late Pleistocene interglacial deposits at Tattershall, Lincolnshire. *Philosophical Transactions of the Royal Society of London, Series B*, 311, 193–236.
- Horsburgh, K., Rennie, A. & Palmer, M. (2020) Impacts of climate change on sea-level rise relevant to the coastal and marine environment around the UK. In: *Marine climate change impacts partnership science review*. Centre for Environment, Fisheries, and Aquaculture Science, pp. 116–131.
- Horton, A. (1989) *Geology of the Peterborough district. Memoir of the British Geological Survey, Sheet 158, England and Wales.* London: HMSO, 44 pp.
- Horton, A., Keen, D.H., Field, M.H., Robinson, J.E., Coope, G.R. & Currant, A.P. et al. (1992) The Hoxnian Interglacial deposits at Woodston, Peterborough. *Philosophical Transactions of the Royal Society of London. Series B*, 338, 131–164.
- Huntley, D.J. & Baril, M.R. (1997) The K content of the K-feldspars being measured in optical dating or in thermoluminescence dating. *Ancient TL*, 15, 11–13.
- Imbrie, J., Hays, J.D., Martinson, D.G., McIntyre, A., Morley, J.J., Pisias, N.G. et al. (1984) The orbital theory of Pleistocene climate: support from a revised chronology of the marine δ<sup>18</sup>O record. In: Berger, A.L., Imbrie, J., Hays, J., Kukla, G. & Saltzman, B. (Eds.) *Milankovitch and climate, Part 1*. Dordrecht: Reidel, pp. 269–305.
- IPCC. (2013) Climate Change 2013: the physical science basis. In: Contribution of Working Group I to the Fifth Assessment Report of the Intergovernmental Panel on Climate Change. Cambridge: Cambridge University Press.
- IPCC. (2023) Climate change 2023: Synthesis report. In: Core Writing Team, Lee, H. & Romero, J. (Eds.) Contribution of Working Groups I, II and III to the Sixth Assessment Report of the Intergovernmental Panel on Climate Change. Geneva: Intergovernmental Panel on Climate Change, pp. 1–34. Available from: https://doi.org/10.59327/IPCC/AR6-9789291691647.001
- Jones, R.W. & Whittaker, J.E. (2010) Palaeoenvironmental interpretation of the Pleistocene–Holocene of the British Isles, using proxy Recent benthonic foraminiferal distribution data. In: Whittaker, J.E. & Hart, M.B. (Eds.) Micropalaeontology, sedimentary environments and stratigraphy: a tribute to Dennis Curry (1912–2001), Special Publication. Bath, London: The Micropalaeontological Society, pp. 261–279.
- Kaufman, D.S. & Manley, W.F. (1998) A new procedure for determining DL amino acid ratios in fossils using reverse phase liquid chromatography. *Quaternary Science Reviews*, 17, 987–1000.
- Keen, D.H. (1990) Significance of the record provided by Pleistocene fluvial deposits and their included molluscan faunas for palaeoenvironmental reconstruction and stratigraphy: case studies from the English Midlands. *Palaeogeography, Palaeoclimatology, Palaeoe*cology, 80, 25–34.
- Keen, D.H., Bateman, M.D., Coope, G.R., Field, M.H., Langford, H.E., Merry, J.S. et al. (1999) Sedimentology, palaeoecology and geochronology of Last Interglacial deposits from Deeping St James, Lincolnshire, England. *Journal of Quaternary Science*, 14, 411–436.

- Keen, D.H., Robinson, J.E., West, R.G., Lowry, F., Bridgland, D.R. & Davey, N.D.W. (1990) The fauna and flora of the March Gravels at Northam Pit, Eye, Cambridgeshire, England. *Geological Magazine*, 127(5), 453–465.
- Keen, D.H., van Vliet-Lanoë, B. & Lautridou, J.-P. (1996) Two long sedimentary records from Jersey, Channel Islands: stratigraphic and pedological evidence for environmental change during the last 200 kyr. *Quaternaire*, 7, 3–13.
- Killeen, I., Aldridge, D. & Oliver, G. (2004) Freshwater bivalves of Britain and Ireland. Telford: Field Studies Council.
- Kopp, R.E., Simons, F.J., Mitrovica, J.X., Maloof, A.C. & Oppenheimer, M. (2009) Probabilistic assessment of sea level during the last interglacial stage. *Nature*, 462, 863–867.
- Kosnik, M.A. & Kaufman, D.S. (2008) Identifying outliers and assessing the accuracy of amino acid racemization measurements for geochronology: II. Data screening. *Quaternary Geochronology*, 3, 328–341.
- Laforge, M. (2012) Le cadre chronostratigraphique des peuplements pléistocènes de l'Ouest de la France. Eustatisme, changements climatiques et occupations humaines. Thèse, Université de Rennes 1.
- Langford, H.E. (1999) Sedimentological, palaeogeographical and stratigraphical aspects of the Middle Pleistocene geology of the Peterborough area, eastern England. PhD Thesis, Anglia Polytechnic University, Cambridge.
- Langford, H.E. (2004) Post-Anglian drainage reorganisation affecting the Nene and the Welland. In: Langford, H.E. & Briant, R.M. (Eds.)
   Nene Valley, Field Guide. Cambridge: Quaternary Research Association, pp. 36–43.
- Langford, H.E. (2012) A comment on the MIS 8 glaciation of the Peterborough area, eastern England. *Quaternary Newsletter*, 127, 6–20.
- Langford, H.E. (2018) Drainage network reorganization affecting the Nene and Welland catchments of eastern England as a result of a late Middle Pleistocene glacial advance. *The Depositional Record*, 4, 177–201.
- Langford, H.E. (2025) Comments on 'Late Middle Pleistocene Wolstonian Stage (MIS 6) glaciation in lowland Britain and its North Sea regional equivalents—a review'. Boreas, in press. doi.org/10.1111/bor.70011
- Langford, H.E., Bateman, M.D., Boreham, S., Knudsen, K.-L., Merry, J. & Penney, D. (2004a) King's Dyke. In: Langford, H.E. & Briant, R.M. (Eds.) *Nene Valley*, Field Guide. Cambridge: Quaternary Research Association, pp. 174–194.
- Langford, H.E., Bateman, M.D., Boreham, S., Fletcher, W., Green, C.,
  Keen, D.H. et al. (2004b) Funtham's Lane East. In: Langford, H.E. &
  Briant, R.M. (Eds.) Nene Valley, Field Guide. Cambridge: Quaternary Research Association, pp. 69–106.
- Langford, H.E., Bateman, M.D., Penkman, K.E.H., Boreham, S., Briant, R.M., Coope, G.R. et al. (2007) Age-estimate evidence for Middle–Late Pleistocene aggradation of River Nene 1st Terrace deposits at Whittlesey, eastern England. *Proceedings of the Geologists' Association*, 118, 283–300.
- Langford, H.E., Boreham, S., Briant, R.M., Coope, G.R., Horne, D.J., Schreve, D.C. et al. (2014b) Middle to Late Pleistocene palaeoecological reconstructions and palaeotemperature estimates for cold/cool stage deposits at Whittlesey, eastern England. *Quaternary International*, 341, 6–26.
- Langford, H.E., Boreham, S., Briant, R.M., Coope, G.R., Horne, D.J., Penkman, K.E.H. et al. (2017) Evidence for the early onset of the Ipswichian thermal optimum: palaeoecology of Last Interglacial deposits at Whittlesey, eastern England. *Journal of the Geological Society*, 174, 988–1003.
- Langford, H.E., Boreham, S., Coope, G.R., Fletcher, W., Horne, D.J., Keen, D.H. et al. (2014a) Palaeoecology of a late MIS 7 interglacial deposit from eastern England. *Quaternary International*, 341, 27–45.
- Langford, H.E. & Briant, R.M. (2004) Post-Anglian deposits in the Peterborough area and the Pleistocene history of the Fen basin. In: Langford, H.E. & Briant, R.M. (Eds.) *Nene Valley*, Field Guide. Cambridge: Quaternary Research Association, pp. 22–35.
- Lea, D.W., Martin, P.A., Pak, D.K. & Spero, H.J. (2002) Reconstructing a 350 ky history of sea level using planktonic Mg/Ca and oxygen isotope records from a Cocos Ridge core. *Quaternary Science Reviews*, 21, 283–293.

1099/1417, D. Downloaded from https://onlinelibrary.wiley.com/doi/10.1002/gs.70025 by NCE, National Institute for Health and Care Excellence, Wiley Online Library on [17/1/12025]. See the Terms and Conditions (https://onlinelibrary.wiley.com/terms-and-conditions) on Wiley Online Library for rules of use. OA articles are governed by the applicable Creative Commons Licenson

- Lefebvre, D. (1993) Different types of ending to the last two interglacials. *Boreas*, 22, 71–76.
- Lisiecki, L.E. & Raymo, M.E. (2005) A Pliocene–Pleistocene stack of 57 globally distributed benthic  $\delta^{18}$ O records. *Paleoceanography*, 20, PA1003. Available from: https://doi.org/10.1029/2004PA 001071
- Long, A.J., Barlow, N.L.M., Busschers, F.S., Cohen, K.M., Gehrels, W.R. & Wake, L.M. (2015) Near-field sea-level variability in northwest Europe and ice sheet stability during the last interglacial. *Quaternary Science Reviews*, 126, 26–40.
- Maddy, D. (1999) English Midlands. In: Bowen, D.Q. (Ed.) *A revised correlation of Quaternary deposits in the British Isles.* Bath: Geological Society Publishing House, pp. 28–44.
- Mahan, S. & DeWitt, R. (2019) Principles and history of luminescence dating. In: Bateman, M.D. (Ed.) *The handbook of luminescence dating*. Dunbeath: Whittles Publishing, pp. 1–39.
- Marine Climate Change Impacts Partnership (undated). Sea level rise. Available from: https://www.mccip.org.uk
- Marr, J.E. & King, W.B.R. (1928) Pleistocene marine gravels at Eye, Northamptonshire. *Geological Magazine*, 65, 210–212.
- Martinson, D.G., Pisias, N.G., Hays, J.D., Imbrie, J., Moore, T.C. & Shackleton, N.J. (1987) Age dating and the orbital theory of the ice ages: development of a high-resolution 0 to 300,000-year chronostratigraphy. *Quaternary Research*, 27, 1–29.
- Meijer, T. & Cleveringa, P. (2009) Aminostratigraphy of Middle and Late Pleistocene deposits in The Netherlands and the southern part of the North Sea Basin. *Global and Planetary Change*, 68, 326–345.
- Meijer, T. & Preece, R.C. (2000) A review of the occurrence of *Corbicula* in the Pleistocene of north-west Europe. *Geologie en Mijnbouw*, 79(2/3), 241–255.
- Millman, E., Wheeler, L., Billups, K., Kaufman, D. & Penkman, K.E.H. (2022) Testing the effect of oxidizing pre-treatments on amino acids in benthic and planktic foraminifera tests. *Quaternary Geochronol*ogy, 73, 101401.
- Monaco, L., Leicher, N., Palladino, D.M., Arienzo, I., Marra, F., Petrelli, M. et al. (2022) The Fucino 250–170 ka tephra record: new insights on peri-Tyrrhenian explosive volcanism, central Mediterranean tephrochronology, and timing of the MIS 8–6 climate variability. Quaternary Science Reviews, 296, 107797.
- Murray, A.S. & Wintle, A.G. (2000) Luminescence dating of quartz using an improved single-aliquot regenerative-dose protocol. *Radiation Measurements*, 32, 57–73.
- Murray, A.S. & Wintle, A.G. (2003) The single aliquot regenerative dose protocol: potential for improvements in reliability. *Radiation Measurements*, 37, 377–381.
- National Oceanography Centre. (2025) UK sea level is rising faster than the global average. Available from: https://noc.ac.uk/news/uksea-level-rising-faster-global-average
- Past Interglacials Working Group of PAGES. (2016) Interglacials of the last 800,000 years. *Reviews of Geophysics*, 54, 162–219.
- Peeters, J., Busschers, F.S., Stouthamer, E., Bosch, J.H.A., Van den Berg, M.W., Wallinga, J. et al. (2016) Sedimentary architecture and chronostratigraphy of a late Quaternary incised-valley fill: a case study of the late Middle and Late Pleistocene Rhine system in the Netherlands. Quaternary Science Reviews, 131, 211–236.
- Penkman, K.E.H. (2005) Amino acid geochronology: a closed system approach to test and refine the UK model. Unpublished PhD Thesis, University of Newcastle.
- Penkman, K., Preece, R.C., Keen, D.H. & Collins, M.J. (2008a) British Aggregates: an Improved Chronology Using Amino Acid Racemization and Degradation of Intra-crystalline Amino Acids (IcPD). Department Report Series 6/2008. English Heritage Research, London. Available at: http://services.english-heritage.org.uk/ResearchReportsPdfs/006\_2008WEB.pdf
- Penkman, K.E.H., Kaufman, D.S., Maddy, D. & Collins, M.J. (2008b) Closed-system behaviour of the intra-crystalline fraction of amino acids in mollusc shells. *Quaternary Geochronology*, 3, 2–25.
- Penkman, K.E.H., Preece, R.C., Bridgland, D.R., Keen, D.H., Meijer, T., Parfitt, S.A. et al. (2011) A chronological framework for the British Quaternary based on *Bithynia* opercula. *Nature*, 476, 446–449.
- Penkman, K.E.H., Preece, R.C., Bridgland, D.R., Keen, D.H., Meijer, T., Parfitt, S.A. et al. (2013) An aminostratigraphy for the British

- Quaternary based on *Bithynia* opercula. *Quaternary Science Reviews*, 61, 111–134.
- Pharaoh, T. (2018) The Anglo-Brabant Massif: persistent but enigmatic palaeo-relief at the heart of western Europe. *Proceedings of the Geologists' Association*, 129, 278–328.
- Preece, R.C. (1995) Mollusca from interglacial sediments at three critical sites in the Lower Thames. In: Bridgland, D.R., Allen, P. & Haggart, B.A. (Eds.) *The Quaternary of the lower reaches of the Thames*, Field Guide. Durham: Quaternary Research Association, pp. 55–60.
- Preece, R.C. & Penkman, K.E.H. (2005) New faunal analyses and amino acid dating of the Lower Palaeolithic site at East Farm, Barnham, Suffolk. *Proceedings of the Geologists' Association*, 116, 363–377.
- Prescott, J.R. & Hutton, J.T. (1994) Cosmic ray contributions to dose rates for luminescence and ESR dating: large depths and long-term time variations. *Radiation Measurements*, 23, 497–500.
- Proctor, C.J. & Smart, P.L. (1991) A dated cave sediment record of Pleistocene transgressions on Berry Head, Southwest England. *Journal of Quaternary Science*, 6(3), 233–244.
- Railsback, L.B., Gibbard, P.L., Head, M.J., Voarintsoa, N.R.G. & Toucanne, S. (2015) An optimized scheme of lettered marine isotope substages for the last 1.0 million years, and the climatostratigraphic nature of isotope stages and substages. *Quaternary Science Reviews*, 111, 94–106.
- Rhodes, E.J. (2015) Dating sediments using potassium feldspar single-grain IRSL: initial methodological considerations. *Quaternary International*, 362, 14–22.
- Roberts, D.H., Evans, D.J.A., Callard, S.L., Clark, C.D., Bateman, M.D., Medialdea, A. et al. (2018) Ice marginal dynamics of the last British-Irish Ice Sheet in the southern North Sea: ice limits, timing and the influence of the Dogger Bank. *Quaternary Science Reviews*, 198, 181–207.
- Robinson, L.F., Henderson, G.M. & Slowey, N.C. (2002) U–Th dating of marine isotope stage 7 in Bahamas slope sediments. *Earth and Planetary Science Letters*, 196, 175–187.
- Rodrigues, T., Alonso-García, M., Hodell, D.A., Rufino, M., Naughton, F., Grimalt, J.O. et al. (2017) A 1-Ma record of sea surface temperature and extreme cooling events in the North Atlantic: a perspective from the Iberian margin. *Quaternary Science Reviews*, 172, 118–130.
- Rohling, E.J., Grant, K., Bolshaw, M., Roberts, A.P., Siddall, M., Hemleben, C. et al. (2009) Antarctic temperature and global sea level closely coupled over the past five glacial cycles. *Nature Geoscience*, 2(7), 500–504.
- Rose, J. (2015) Pleistocene fluvial deposits and soils. In: Lee, J.R., Woods, M.A. & Moorlock, B.S.P. (Eds.) *British regional geology: East Anglia*, 5th edn. Keyworth: British Geological Survey, pp. 130–145.
- Sánchez-Goñi, M.F., Eynaud, F., Turon, J.-L. & Shackleton, N.J. (1999) High resolution palynological record off the Iberian margin: direct land–sea correlation for the last interglacial complex. *Earth and Planetary Science Letters*, 171, 123–137.
- Satow, C., Grant, K.M., Wulf, S., Schulz, H., Mallon, A., Matthews, I. et al. (2020) Detection and characterisation of Eemian marine tephra layers within the Sapropel S5 sediments of the Aegean and Levantine Seas. *Quaternary*, 3(1), 6.
- Shackleton, N.J. (1969) The last interglacial in the marine and terrestrial record. *Proceedings of the Royal Society of London Series B*, 174, 135–154.
- Shackleton, N.J., Chapman, M., Sánchez-Goñi, M.F., Pailler, D. & Lancelot, Y. (2002) The classic marine isotope substage 5e. *Quaternary Research*, 58, 14–16.
- Shackleton, N.J., Sánchez-Goñi, M.F., Pailler, D. & Lancelot, Y. (2003) Marine isotope substage 5e and the Eemian interglacial. *Global and Planetary Change*, 36, 151–155.
- Shennan, I. (1982) Interpretation of Flandrian sea-level data from the Fenland, England. *Proceedings of the Geologists' Association*, 93(1), 53–63.
- Siddall, M., Abe-Ouchi, A., Andersen, M., Antonioli, F., Bamber, J.L., Bard, E. et al. (2010) The sea level conundrum: case studies from palaeo-archives. *Journal of Quaternary Science*, 25, 19–25.

- Siddall, M., Rohling, E.J., Almogi-Labin, A., Hemleben, C., Meischner, D., Schmelzer, I. et al. (2003) Sea level fluctuations during the last glacial cycle. *Nature*, 423, 853–858.
- Sier, M.J., Peeters, J., Dekkers, M.J., Parés, J.M., Chang, L., Busschers, F.S. et al. (2015) The Blake Event recorded near the Eemian type locality—a diachronic onset of the Eemian in Europe. *Quaternary Geochronology*, 28, 12–28.
- Skertchly, S.B.J. (1877) The geology of the Fenland. Memoir of the Geological Survey of Great Britain. London: HMSO.
- Sparks, B.W. & West, R.G. (1970) Late Pleistocene deposits at Wretton, Norfolk. I. Ipswichian Interglacial deposits. *Philosophical Transactions of the Royal Society of London, Series B: Biological Sciences*, 258(818), 1–30.
- Spooner, N.A. (1994) The anomalous fading of infrared-stimulated luminescence from feldspars. *Radiation Measurements*, 23, 625–632.
  Spratt, R.M. & Lisiecki, L.E. (2016) A Late Pleistocene sea level stack. *Climate of the Past*, 12, 1079–1092.
- Straw, A. (2018) Geomorphology of the Kirmington interglacial deposits and the Immingham channel, north Lincolnshire. *Mercian Geologist*, 19(3), 133–140.
- Sykes, G.A., Collins, M.J. & Walton, D.I. (1995) The significance of a geochemically isolated intra-crystalline organic fraction within biominerals. *Organic Geochemistry*, 23, 1059–1065.
- Thomas, G.N. (2001) Late Middle Pleistocene pollen biostratigraphy in Britain: pitfalls and possibilities in the separation of interglacial sequences. *Quaternary Science Reviews*, 20, 1621–1630.
- Thompson, W.G. & Goldstein, S.L. (2005) Open-system coral ages reveal persistent suborbital sea-level cycles. *Science*, 308, 401–404.
- Turner, C. (1973) Eastern England. In: Mitchell, G.F., Penny, L.F., Shotton, F.W. & West, R.G. (Eds.) A correlation of Quaternary deposits in the British Isles, Special Report 4. London: Geological Society, pp. 8–18.
- Ventris, P.A. (1996) Hoxnian Interglacial freshwater and marine deposits in northwest Norfolk, England and their implications for sea-level reconstruction. Quaternary Science Reviews, 15, 437–442.
- Waelbroeck, C., Labeyrie, L., Michel, E., Duplessy, J.C., McManus, J.F., Lambeck, K. et al. (2002) Sea-level and deep water temperature changes derived from benthic foraminifera isotopic records. *Quaternary Science Reviews*, 21, 295–305.
- Wendt, K.A., Li, X., Edwards, R.L., Cheng, H. & Spötl, C. (2021) Precise timing of MIS 7 substages from the Austrian Alps. *Climate of the Past*, 17(4), 1443–1454.
- West, R.G. (1987) A note on the March Gravels and Fenland sea levels. *Bulletin of the Geological Society of Norfolk*, 37, 27–34.
- West, R.G., Andrew, R., Catt, J.A., Hart, C.P., Hollin, J.T., Knudsen, K.L. et al. (1999) Late and Middle Pleistocene deposits at Somersham, Cambridgeshire, UK: a model for reconstructing fluvial/estuarine depositional environments. *Quaternary Science Reviews*, 18(11), 1247–1314.
- West, R.G., Andrew, R., Knudsen, K.L., Peglar, S.M. & Petit, M.E. (1995b) Late Pleistocene deposits at Chatteris, March and Wimblington, Cambridgeshire, England. *Proceedings of the Geologists' Association*, 106, 195–210.
- West, R.G., Knudsen, K.L., Penney, D.N., Preece, R.C. & Robinson, J.E. (1994) Palaeontology and taphonomy of Late Quaternary fossil assemblages at Somersham, Cambridgeshire, England, and the problem of reworking. *Journal of Quaternary Science*, 10, 285–310.
- West, R.G., Peglar, S.M., Pettit, M.E. & Preece, R.C. (1995a) Late Pleistocene deposits at Block Fen, Cambridgeshire, England. *Journal* of Quaternary Science, 10, 285–310.
- Wheeler, L.J. (2022) Towards an aminostratigraphy of foraminifera for Pleistocene sea-level records: testing the intra-crystalline approach to amino acid racemisation dating. PhD Thesis, University of York.
- White, T.S., Bridgland, D.R., Westaway, R. & Straw, A. (2017) Evidence for late Middle Pleistocene glaciation of the British margin of the southern North Sea. *Journal of Quaternary Science*, 32, 261–275.
- Whittaker, J.E., Horne, D.J. & Lord, A. (2005) New microfaunal data from the Raincliff Formation (Speeton Shell Bed), North Yorkshire. *Quaternary Newsletter*, 107, 20–23.

## Appendix A: Counts of foraminifera for unsuccessful AAG dating attempts

Foraminifera AAG dating attempts (AAG-U1-AAG-U3, Fig. 2) were made for facies FI at KD4 (King's Dyke) and facies Gcm/ Fm and Gt-St at WF3 (West Face) but were considered unsuccessful because they yielded [I-Ser]/[I-Asx] > 0.8 (Wheeler, 2022, unpublished data). Material supplied by HEL but not used has been identified and counted by KLK. As the picked material is biased toward the selection of larger specimens of Haynesina germanica, Ammonia spp. and Elphidium spp., the counts cannot be used in any quantitative sense because they do not represent true assemblages. As there are no previously published accounts of foraminifera for these sedimentary facies at sections KD4 and WF3, the counts for the used and unused material for foraminifera AAG dating are provided below, and species not previously identified have been added (in parentheses) to the counts in Table 5(a). At WF3, only the count for facies Gt-St is appropriate, as the foraminifera in that facies are considered to be reworked from underlying facies Sm. Qualitative assessment of the counts for facies Fl at KD4 and Sm at WF3 indicates that they are not in conflict with the interpreted depositional environment of the estuarine-marine microfauna. As only unpublished preliminary data were available (from material supplied from samples analysed for molluscs) on the foraminifera present at the base of facies Gcm/Fm, the count for that facies is also included in the table below and can be used to qualitatively assess the depositional environment of the foraminifera fauna.

	Fac Fl, k		Fac Gt–St,		Facies Gcm/ Fm (base), WF3		
Таха	Not used	Used	Not used	Used	Not used	Used	
Elphidium williamsoni	48		30		32		
Haynesina germanica	100	850	114	150	121	650	
Aubignyna perlucida			2		4		
Elphidium clavatum/E. selseyensis	46		34		82		
Elphidium gerthi					2		
Elphidium magellanicum	1		1		17		
Haynesina depressula	1		1		7		
Cibicides lobatulus	2				1		
Cibicides sp.					1		
Elphidium incertum	4		1		2		
Elphidium albiumbilicatum	4		8		4		
Elphidium spp.		50					
Cassidulina reniformis					1		
Ammonia spp.	114	50	24		53		
Lagena spp.					1		
Oolina spp.					1		
Bolivina spp.					1		
Fissurina sp.					1		
Rosalina sp.					1		
Stainforthia fusiformis	1						
Buccella frigida calida	6		1		2		
Elphidium gunteri			2		5		
Nonion pauperata					2		
Inderminata	9				2		
Totals	338	950	215	150	343	650	

# Appendix B: Information provided by ostracods picked from samples used for unsuccessful foraminifera AAG dating attempts

Ostracods were also picked from samples AAG-U2 and AAG-U3 used for foraminifera dating attempts (Fig. 2); none were found in AAG-U1. The AAG-U2 material (in parentheses in the table below) suggested a mixed and size-sorted estuarine taphocoenosis dominated by juveniles of freshwater, brackish and possibly marine genera. Only three adult valves were found, two of Cyprideis torosa and one of Candona sp. Small juveniles of C. torosa and Candona sp. were quite numerous, together with juveniles tentatively identified as Leptocythere sp., Cytheromorpha sp., Hirschmannia sp., Cytheropteron sp., Hemicytherura sp., Semicytherura sp., Ilyocypris sp. and Darwinula sp., among others. When added to the material in the following table, previously identified from an unpublished molluscan sample, an assemblage dominated by brackishwater C. torosa together with freshwater Neglecandona neglecta and Ilyocypris sp. is apparent. The overall assemblage composition still suggests an estuarine taphocoenosis that was transported, mixed and size-sorted by tidal currents, but including a relatively abundant suite of adults and juveniles of C. torosa that could represent a thanatocoenosis in situ. The noteworthy occurrence of adult valves of the freshwater ostracod Psychrodromus olivaceus, which inhabits springs and spring seepages, could be explained as evidence of a spring on the margin of the estuary. It should be noted, however, that as the material was provided from separate coarse and fine fractions of a sediment sample, the counts should not be used in any quantitative sense because they are not representative of a true assemblage.

As with the original microfaunal analysis of facies Fl at KD4, the ostracod material from AAG-U3 was not very useful. There was only one whole valve (a juvenile), the rest being broken fragments of valves. Due to the fragmentary nature, the material could not be identified with certainty, but the whole juvenile valve and most of the fragments could be *Prionocypris zenkeri*, and two broken valves appear to be *Candona* sp. This could suggest a freshwater assemblage.

Таха	Facies Gcm/Fm (base), WF3 Valves
Marine/outer estuarine ostracods	
Hemicythere villosa	1
Cytheropteron sp. juvenile.	(2)
Hemicytherura sp. juvenile	(2)
Semicytherura sp. juvenile	(1)
Hirschmannia sp. juvenile	(2)
Brackish ostracods	
Cyprideis torosa (smooth)	58
Cytheromorpha fuscata	2 (1)
Leptocythere sp. juvenile	(7)
Freshwater ostracods	
Ilyocypris spp.	28
Candona candida	4
Neglecandona neglecta	32 (1)
Candona sp. juvenile	(18)
Pseudocandona sp.	1
Herpetocypris sp.	10
Cyclocypris spp.	5
Heterocypris salina	4
Psychrodromus olivaceus	10
Darwinula sp. juvenile	(3)
Total ostracods	157 (37)